UNITED NATIONS
UNIVERSITY

GEOTHERMAL TRAINING PROGRAMME
Orkustofnun, Grensasvegur 9,
IS-108 Reykjavik, Iceland

Reports 2011
Number 20

BOREHOLE GEOLOGY AND HYDROTHERMAL MINERALISATION OF WELL HE-32, HELLISHEIDI GEOTHERMAL FIELD, SW-ICELAND

Isa Lugaizi
Ministry of Energy and Mineral Development
Department of Geological Survey and Mines
P.O. Box 9 Entebbe
UGANDA
isalugayizi@yahoo.com

ABSTRACT

Well HE-32, is an exploration/production well at the base of Mt. Skardsmýrarfjall mountain in the Hellisheidi high-temperature field, within the Hengill volcanic system, in SW-Iceland. It is a directional well drilled to 2465 m depth. The lithology of the uppermost 1116 m has been analysed through petrographic examination of cuttings (binocular and optical microscopy) and geophysical logs. It shows that the lithology is predominantly a hyaloclastite formation comprised of pillow basalts, basaltic breccia and basaltic tuff. Additionally, a few thin interglacial lava flows are present. A couple of thin layers of fine- to medium-grained tholeiitic basalt intrusions occur around 10, 200 and 550 m. A prediction of the lithology for the interval 1116-1900 m was undertaken demonstrating how geophysical logging can be of value where cuttings are missing due to circulation losses, yet giving an indication of the lithology is vital, e.g., in the production (liner) part of the well. Eight boundaries within 4 rock units were inferred from these logs. Hydrothermal alteration is controlled by temperature, rock type and permeability. The mineral assemblages showed that the alteration temperature increased with depth, first with the appearance of minerals such as low-temperature zeolites, quartz, and smectite. The alteration was high below 388 m with the appearance of quartz (≥180°C), wairakite (≥200°C) and later epidote (≥230°C) at 690 m. The alteration increased below 850 m (with the appearance of actinolite, ≥280°C) and localized at around 1084 m (+garnet, ≥300°C). Abundant prehnite at 700-1100 m depth may be due to low permeability. Five temperature related alteration zones were characterised: smectite-zeolite zone (0-275 m), mixed-layer clay zone (275-375 m), chlorite zone (375-690 m), chlorite-epidote zone (690-850 m) and epidote-actinolite zone (850-1116 m). Five feed zones/aquifers were identified using temperature logs and drillers' logs. These show an association with lithological boundaries and intrusive bodies. Comparison of alteration mineral temperature and formation temperature show that the geothermal system is overall in equilibrium, with a reservoir temperature of 230-270°C down to ~850 m, although temperatures of up to 300°C were recorded in a few fluid inclusions. At deeper levels, a localized ~40°C cooling at the aquifer zones between 1000-1100 m was observed. A comparison of the three wells HE-3, HE-32 and HE-51, all located on the same well pad, has enhanced our understanding that while relationships in overall subsurface geology and hydrogeology may exist in adjacent wells, each well is independent and behaves as an individual.

1. INTRODUCTION

The principal work of geologists in geothermal exploration traditionally was to discover and map the surface geological structures and measure surface stratigraphic sections. Many wells were drilled without the benefit of a geologic appraisal of the area, and representative samples were not saved for later studies (Low, 1977). Little or no thought was given to subsurface work as a basic approach to geothermal exploration. Nowadays, geologists are concerned with subsurface geology; the main subsurface geologic data comes from well cuttings, cores and geophysical logs. The quality of well cuttings has steadily improved as a result of improved drilling practices, which have encouraged greater emphasis on subsurface analysis. Thus, the borehole geologist occupies a foremost position in the search for new geothermal fields, although surface field geology still maintains an important role in all exploration and exploitation programs. The subsurface geologists have to work in synchronous harmony with other disciplines to produce the desired output; therefore, teams of drilling engineers, reservoir engineers, fluid chemists/geochemist, geophysicists, environmental scientists and others work together seamlessly for a successful geothermal project.

The author of this report participated in the 6-month United Nations University (UNU) geothermal training programme at Iceland GeoSurvey (ISOR) in Iceland, specialising in borehole geology. The second half of the training consisted of the study presented here. The aim was to understand the natural geothermal conditions of well HE-32 through studying the subsurface geology, mainly the mineralogy and rock types of the geological units drilled through to define the stratigraphy and structures within the well. Furthermore, it was intended for the author to become acquainted with the type, extent and relative amount of overall alteration within the well, relative amounts and mineralogy of the veining and open space filling. This leads to an enhanced understanding of the water-rock interaction and hydrothermal alteration, the location of permeable zones, and to define the hydrological connection between the studied well and HE-3 and HE-51 drilled on the same well pad.

2. GEOLOGY AND GEOTHERMAL ACTIVITY IN ICELAND

2.1 Brief regional geology of Iceland

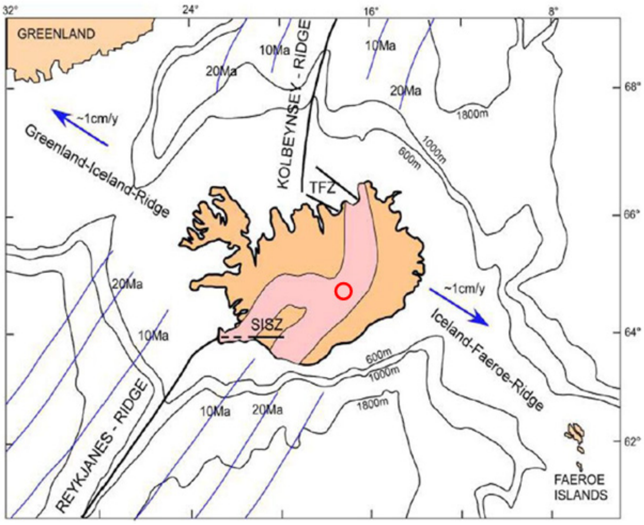

FIGURE 1: Location of Iceland in relation to the American and the Eurasian plate and the elevated Greenland–Iceland–Faeroes Ridge; note the location of the mantle plume in the red circle. Rift axes are shown in pink (modified from Björnsson et al., 2007)

Iceland is unique in its location across the diverging Mid-Atlantic Ridge, which characterizes the plate boundary of the American and the Eurasian plates, and the elevated Greenland–Iceland–Faeroes Ridge where the asthenospheric flow under the NE Atlantic plate boundary interacts and mixes with a deep-seated mantle plume (Figure 1). These two dynamic systems combine fundamental factors that promote magmatism and tectonics, resulting in one of the most active and productive sub aerial regions on Earth, with an eruption frequency of more than 20 events per century and a magmatic output rate of about 8 km^3 per century in historic times, i.e. over the last 1100 years (Thórdarson and Höskuldsson, 2008).

The Reykjanes Ridge in southwest Iceland and the Kolbeinsey Ridge to the north are segments of the Mid-Atlantic-Ridge. The half-spreading rate is around 1 cm/y, indicated by blue arrows in Figure 1. Magnetic anomalies (blue lines) indicate the increasing age, in millions of years (Ma), of the oceanic floor with increasing distance from the rift axes. Also, the volcano-tectonic rift zones crossing Iceland from southwest to northeast are shown in pink in Figure 1. The South Iceland Seismic Zone (SISZ) in the south and the Tjörnes Fracture Zone (TFZ) in the north are transform zones which connect the volcanic rift zones in Iceland to the segments of the Mid-Atlantic-Ridge (Trønnes, 2002).

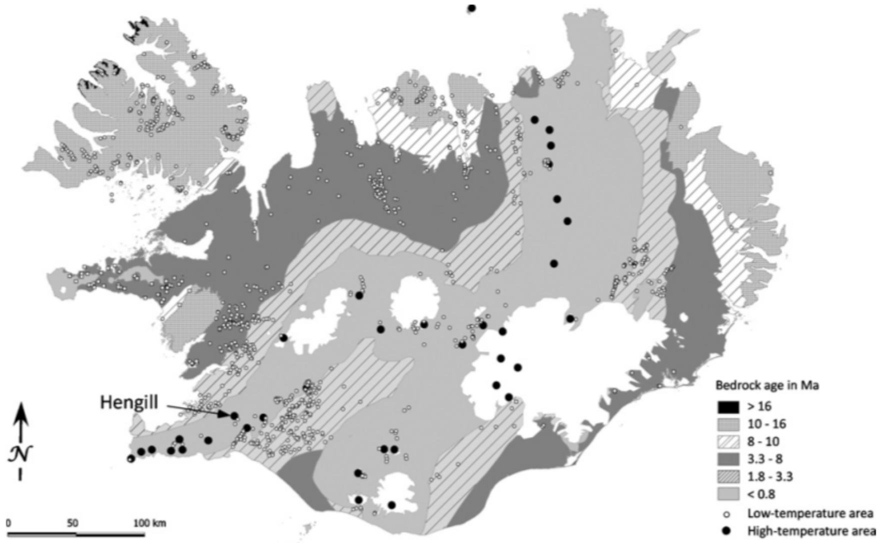

FIGURE 2: A simplified geological and geothermal map of Iceland; white areas are glaciers (from Árnason et al., 2010)

Iceland is located above a mantle plume which is hypothesised to be the cause of its formation through the emission of volcanic material, created by rifting and crustal accretion along the NE-SW axial rift system (e.g. Saemundsson, 1979). It is not surprising, therefore, that the geology is such that the oldest rocks are found to the east and the west and the youngest in the central rifting zone (Figure 2). The surface geology is entirely made up of volcanic rocks with basalts being 80-85% of the volcanic pile, and acid and intermediate rocks 10%. The basalts themselves can be classified into three main types: the compound flows of olivine tholeiite, simple tholeiite (with little or no olivine) and porphyritic basalt with plagioclase and pyroxene. Various investigations have shown that the type of effusion is dependent upon the volcanic zone from which it emerges. The zones, volcanic rift zones and volcanic flank zones are categorised according to the degree of mantle melting. The former are associated with tholeiitic basalts and their derivatives whereas the latter give rise to transitional-alkaline through to alkaline rocks (Jakobsson et al., 2008).

2.2 The geothermal systems of Iceland

Bödvarsson and Pálmason (1961) divided the geothermal systems in Iceland into high-temperature and low-temperature areas (Figure 3). The active volcanic zones are characterized by high heat-flow and extensive geothermal activity. The high-temperature reservoirs have reservoir temperatures between 200 and 400°C and are confined to volcanic systems (Figure 2), in particular the central volcanoes, and are subject to strong tectonic control. The heat source is considered to be magmatic associated with shallow level crustal magma chambers or dyke swarms or, in general, by cooling intrusions (Figure 3). In all the high-temperature areas the dominant rock formations are basaltic hyaloclastic rocks and basalt lavas, but there are also silicic rock formations, for example rhyolites (Saemundsson, 1979). The prevalent permeability, in general, seems to be affiliated with intrusive bodies and sub-vertical faults and fractures. Solfataras and mud pools indicate that the area is a high-temperature zone, which can typically be connected to the phenomena of sulphur precipitation and rock alteration. Additionally, a high concentration of dissolved solids and volcanic gases in the geothermal fluids are indicators of these high-temperature fields (Marosvölgyi, 2009).

On the other hand, the low-temperature areas, also known as medium- and low-enthalpy geothermal systems (Figure 3) are found outside the volcanic zones. Their temperature is, by definition, below 150°C at 1 km depth. The heat source is the surrounding rocks and the hot water circulating in the

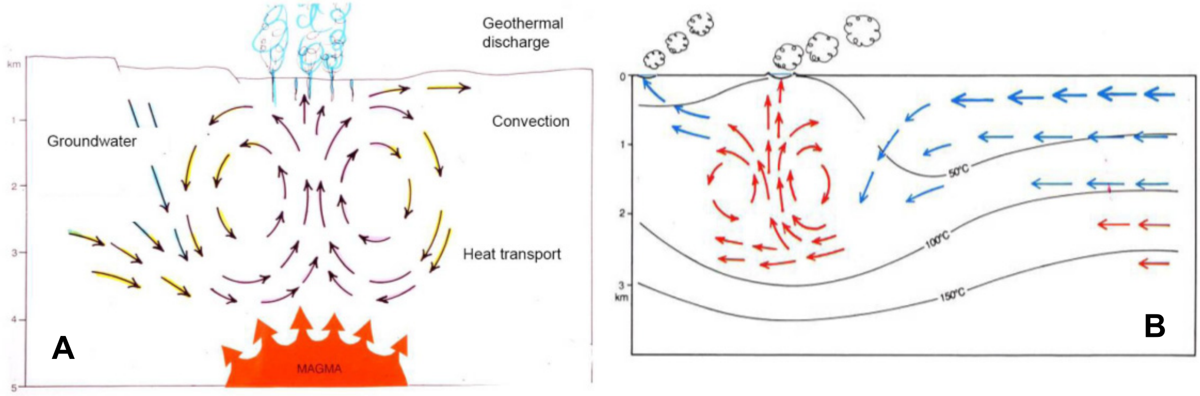

FIGURE 3: a) High-temperature; and b) low-temperature geothermal systems (Björnsson et al., 1990)

faults and fissures (e.g. Björnsson et al., 1990). The geothermal fluid is generally water of meteoric origin with a comparatively low content of dissolved solids and alkaline compounds. The meteoric water first percolates down into the underground rocks where it is warmed up. Convection starts due to the difference in density between the hot and cold water, and steam emerges up to the surface. In these low-temperature areas the dominant rock formations are, but not exclusively, Quaternary and Tertiary rock formations younger than 3.1 M.y.

2.3 Geology and tectonic setting of the study area

The current study was carried out on well HE-32, a directional well drilled to 2465 m in the Hellisheidi high-temperature field which is part of the 112 km^2 greater Hengill geothermal region in SW-Iceland (Figure 2).

2.3.1 Geology

The Hellisheidi high-temperature field is part of the Hengill volcanic system (Figure 2). It is situated in the southern sector of the Hengill central volcano south of the Nesjavellir high-temperature field. The Hengill region is located at a triple junction where two active rift zones meet a seismically active transform zone. The geology of the Hengill volcanic system has been intensely studied (Saemundsson, 1995; Franzson et al., 2010; Hardarson et al., 2010a). The largest part of the volcano is built up of hyaloclastite formations erupted during glacial times, while interglacial lavas erupted in the highlands have flowed to the surrounding lowlands. Intermediate and acid rocks are found on the western edge of the volcano, but have also been found as intrusives in the drill holes throughout the geothermal fields (Saemundsson, 1995; Franzson et al., 2010). Three lava eruptions have been recorded in Holocene time, nine, five and two thousand years ago (Saemundsson, 1995; Franzson et al., 2010). Surface thermal alteration is extensive, being most common in the Hengill mountain in the centre of the volcano, but is evident throughout the volcano. Most of the alteration patches show a clear relationship to tectonic faults and fissures. However, they are often fossilised, indicating a more active system in the past. Surface geothermal activity is common though (Figure 4) as witnessed by the author during a field visit to the study area.

2.3.2 Tecto-seismic setting

The Hengill triple junction is a complex of fissure swarms, partly shown in Figure 4. It is equally a very seismically active area. The last major earthquake episode associated with the Hengill fissure swarm occurred in 1789 with a significant subsidence along the graben faults. Intense seismic activity occurred in 1991-2001 which appeared to be associated with transform tectonic activity related to the South Iceland Seismic Zone (SISZ). Khodayar and Franzson (2007) studied the fracture pattern from aerial photographs with the result that they depicted a similar combination of fracture directions which contributed to the conclusion made by other studies that the Hengill volcanic system is located at a triple junction. This affects the permeability in the crust, discussed in detail by Franzson (2000).

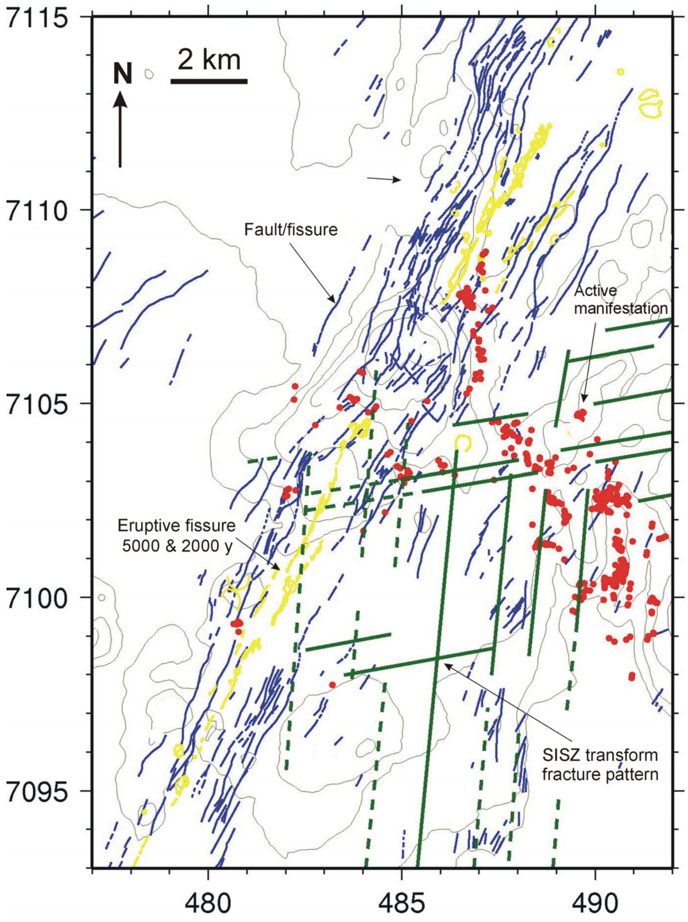

FIGURE 4: The Hengill volcanic system showing the topography, the faults related to the transform system (SISZ), and the post-glacial eruptive fissure swarm cutting the central volcano (from Franzson et al., 2010); the dominant NNE-SSW trend of fissures and faults is shown in blue, green lines are interpreted from seismic data, and red dots show surface manifestations

2.4 Previous studies and research done in the study area

Large-scale utilization of geothermal resources in the Hengill geothermal region dates back to 1990, when Reykjavík Energy (OR) commissioned a 120 MWe and 100 MWt hot water plant at Nesjavellir, north of Mount Hengill, with the water intended for space heating of the city of Reykjavik and surrounding communities. Since then, hot water production has been increased to 290 MWt. In 2006, the first phase of the Hellisheidi power plant, built and operated by OR, south of Mount Hengill was commissioned with an installed capacity of 90 MWe.

The Hellisheidi plant has been built in stages, 133 MWe was on-line in 2007, 90 MWe were added in 2008 and 90 MWe in 2011. It is now generating 303 MWe. In other words, the total installed power production capacity in the Hengill geothermal area is now 423 MWe. Geothermal exploration in the Hengill region had been intermittently going on from the 1940s until the 1980s when it was intensified in preparation for the Nesjavellir plant (Árnason et al., 2010).

2.4.1 Sub-surface exploration

Franzson et al. (2010) described the exploration drilling in the Hengill system which started at Nesjavellir in 1965 with five wells and continued in 1981-1985 with the drilling of 13 wells. A further 10 wells have been drilled as step out and make up wells, along with a few shallower reinjection wells. Drilling exploration of the Hellisheidi field started with a well at Kolvidarhóll in 1986 while a major exploration effort commenced in Hellisheidi in 2001; to date, 57 production wells have been drilled in the area along with 17 reinjection wells, most of them deep (>2000 m). Contrary to Nesjavellir field where vertical wells dominate, directional wells prevail in the Hellisheidi geothermal field where up to four wells are drilled from each drill pad.

2.4.2 Geophysical exploration

Structures and the characteristics of the geothermal system in the Hengill area have been defined by several geophysical exploration methods at different times, for example through: seismic refraction

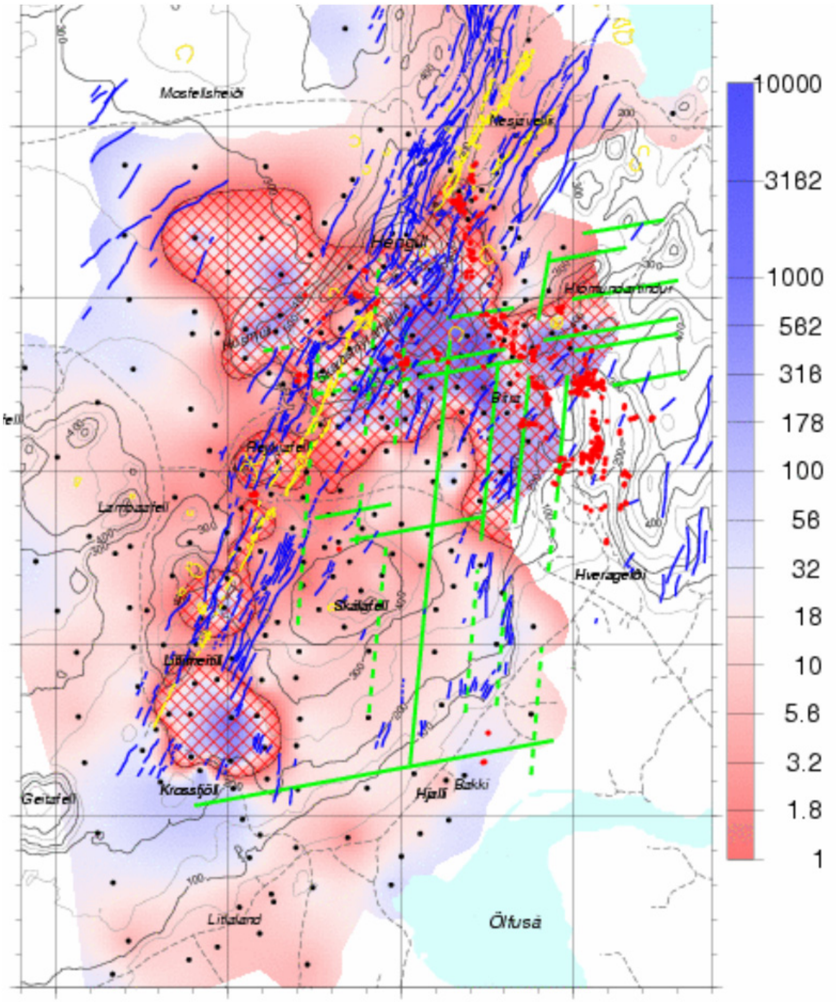

FIGURE 5: A resistivity map of the Hengill central volcano at 850 m b.s.l. showing variations in resistivity; the cross-hatched areas define high-resistivity cores below low resistivity, and are interpreted to indicate alteration temperatures of over 230°C (Árnason et al., 2010)

and passive seismic surveys, aeromagnetic survey, Bouguer gravity survey, Schlumberger and dipole-dipole surveys and magnetotelluric and TEM surveys (e.g. Árnason et al., 2010). While integration of several geophysical methods is important in any geothermal exploration project, it is worth mention that the most informative exploration method in defining the geothermal reservoir prior to drilling is resistivity (e.g. Franzson, 2000). In Iceland, the main emphasis in geophysical exploration of high-temperature geothermal resources is on mapping the resistivity structures and inferring the geothermal alteration mineralogy pattern in the upper 0.5-1 km of the crust by using TEM soundings and the deeper part with magnetotelluric measurements. The reason is that mapping the resistivity structure with these soundings has been proven to be effective in delineating geothermal reservoirs (Árnason et al., 2010).

Árnason et al. (2000) related the resistivity structures to variations in hydrothermal alteration which appear to be of greater importance than the temperature variation. The low-temperature clay-rich outer margin of a high-temperature reservoir is characterized by low resistivity, and the underlying higher resistivity is associated with the formation of chlorite and less water-rich alteration mineral assemblages. Figure 5 shows a resistivity map at 850 m b.s.l. in the Hengill area.

3. BOREHOLE GEOLOGY

Exploration drilling and subsequent geological, geophysical, geochemical and other evaluations of a geothermal well comprise one of the exploration steps to be taken before any production drilling is conducted in a geothermal field. The vertical and horizontal extent of the geothermal reservoir, its thermal and hydrological characteristics, and the structures controlling the flow of geothermal fluids can be predicted by drilling exploration wells into the geothermal system. Based on the information gained from different surface and subsurface explorations, one or more exploration boreholes is drilled depending on the geological complexity of the area and other factors, before drilling for production wells is conducted. Well HE-32 is one of the exploration wells drilled to explore the geothermal reservoir; it appears to be connected to fractures and faults to the northeast where some surface manifestations can be found (Figure 6). It was turned into a production well and is currently producing about 8 MWe at 8 bar pressure.

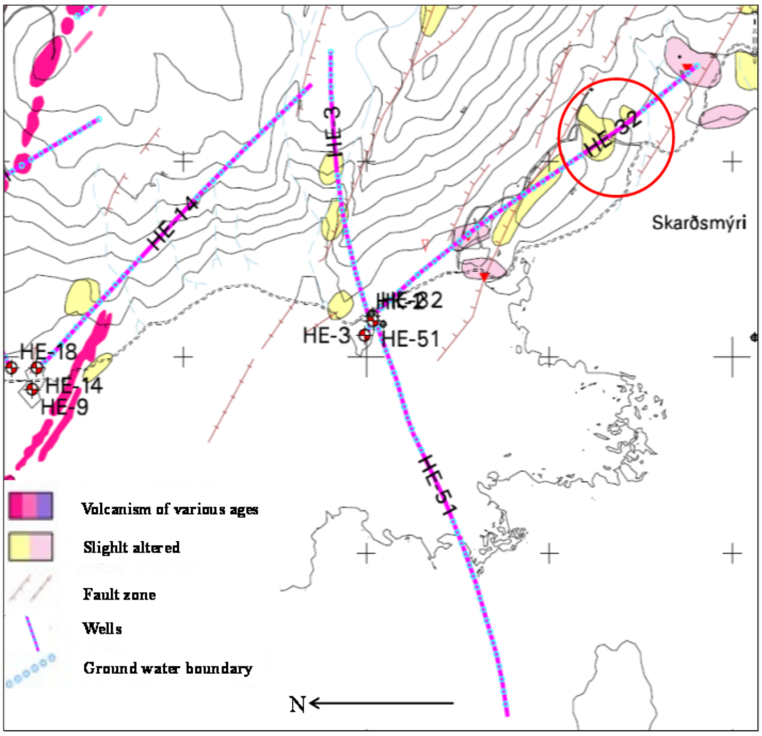

FIGURE 6: The location and direction of well HE-32 (red circle) at Hellisheidi; note also the locations of wells HE- 3 and HE-5 (ISOR data, unpublished)

3.1 Methodology of analysis and scope of the study

In general, the location and characterisation of a subsurface geothermal system requires not only sample collection, preparation, storage and examination, but also thorough knowledge of the local and regional geology, drilling technology, and the full range of potential borehole contaminants. Subsurface geology studies are, therefore, wide and extensive. As such, the methods to be applied depend on the nature and scope of the study to be undertaken.

This study was accomplished by integrating a multitude of different but complimentary methods, schematically summarized in Figure 7. Details of the methods and some procedures for laboratory analyses for X-ray diffractometry are attached in Appendix I.

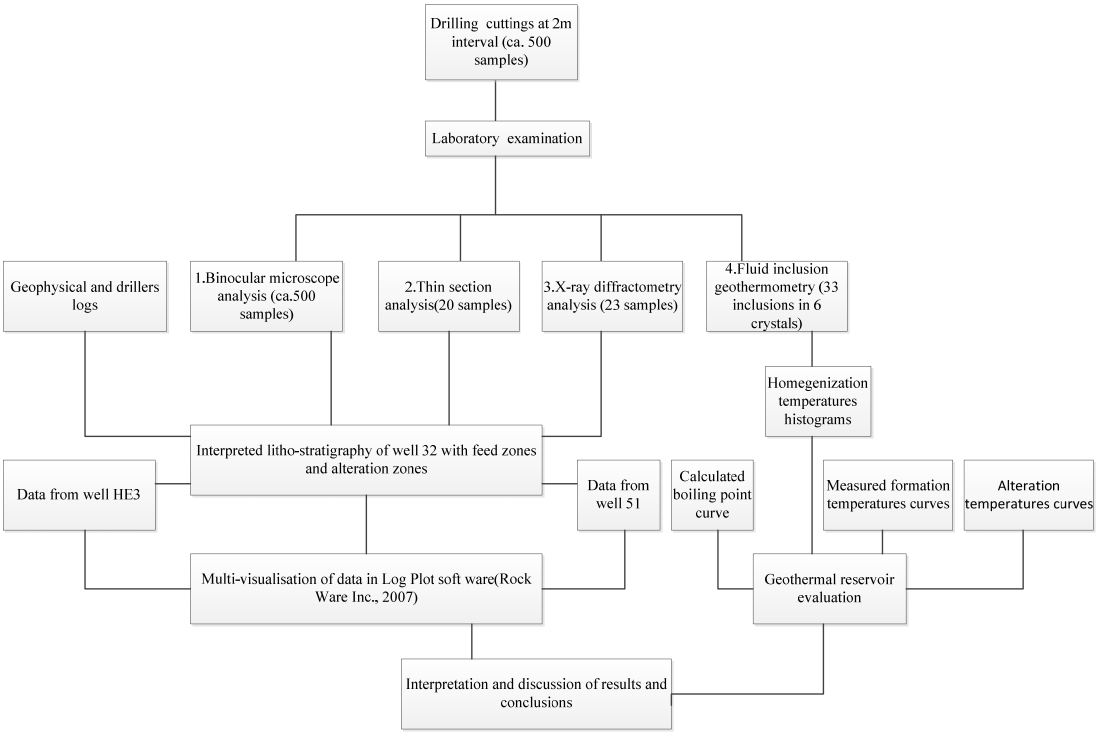

FIGURE 7: Schematic representation of the methods used in the current investigation

3.2 Drilling of well HE-32

Well HE-32 is located in Hellisheidi geothermal field just beneath the southeast slopes of Mt. Skardsmýrarfjall, on the same well pad as wells HE-3 and HE-51 (Figure 7). Its location coordinates, according to the country system (ISN93), are: X = 386016.54 Y = 395104.53 Z = 384 m above sea level. The well was designed as a directional well with bearing N50°A. The build-up of the slope was intended to be 2.5°/30 m, meant to stop when the slope reached 30°. KOP was to commence about 20 m below the safety casing. The well was expected to have entered the reservoir below 500 m depth. The plan was to drill to 2500 m measured depth (just over 2200 m vertical depth). The production casing was to reach about 750 m depth. The design of the well took into account the conditions in well HE-3 which showed a rather shallow alteration compared to other wells in the Hellisheidi production area (Hardarson et al., 2010b). Temperature measurements in HE-3 indicated that 220°C was reached at 500 m depth, 240°C at 700 m and 250°C at 800 m depth. The highest temperature, around 275°C, was reached at around 1200 m measured depth. Below that point, there was a reversal in temperature so that 230°C was measured at 1800 m depth. It was believed that well HE-3 would cut through a fault in Mt. Skardsmýrarfjall at 1200 m depth, and it is possible that the temperature reversal is connected to the patch to the west. Due to the improbable location/direction of well HE-32, it does not cut through the same faults as well HE-3, but rather through other faults that are located farther south and east (Figure 6); therefore, it was uncertain if the temperature reversal was connected to them (Hardarson et al., 2010b; Hardarson et al., 2010c).

3.2.1 Drilling history of well HE-32

The well has a wide diameter and its design is shown in Figure 8. The drilling work was divided into pre-drilling and three stages (Table 1 and Figure 8). In general, the drill rig Saga was used for pre-drilling in May 2007 with a 26" drill bit. It drilled to 97.8 m depth and subsequently a 22 ½" casing was placed in the well. The drill rig Geysir was moved to the site in the beginning of July in order to drill the 1st, 2nd, and 3rd stages.

The 1st stage was drilled with a 21" drill bit down to 307 m depth and an 18⅝" casing was placed to a depth of 306 m, which is the safety casing of the well (Table 1, Figure 9). The well was drilled directionally with a 17 ½" drill bit down to 752 m depth during the 2nd stage and a 13⅜" casing was placed in it. The well was drilled with a 12 ¼" drill bit down to a depth of 2465 m during the 3rd stage and a liner was inserted to the bottom. Casing depths were determined by the site geologist in cooperation with Reykjavik Energy. The drill work was done by Jardboranir Ltd., drilling inspection was done by VGK Ltd. (now Mannvit Eng.) and ÍSOR - Iceland GeoSurvey was contracted for the exploration part and geothermal consultancy.

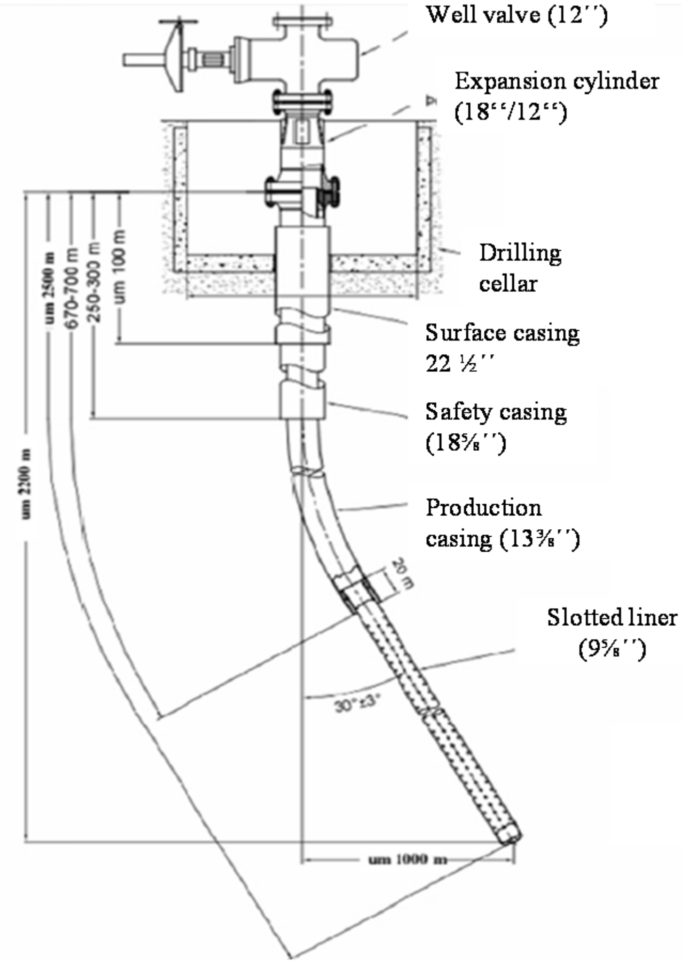

FIGURE 8: Well design of well 32 (Hardarson et al., 2010b)

TABLE 1: Drilling rigs, stages, depth, drill bit size and casing size, type and depth of well HE-32 (Hardarson et al., 2010b; c)

Drill rig	**Stage**	**Drill bit (″)**	**Drilling depth (m)**	**Casing size (″) and type**	**Casing depth (m)**	**Height of drill pad (m)**
Saga	Pre-drilling	26	97.8	22 ½ Surface	96.5	2
Geysir	1st Stage	21	307	18 ⅝ Safety	306	6.8
Geysir	2nd Stage	17 ½	752	13⅜ Production	751.7	6.8
Geysir	3rd Stage	12 ¼	2465	9 ⅝ Liner	646-2448	6.8

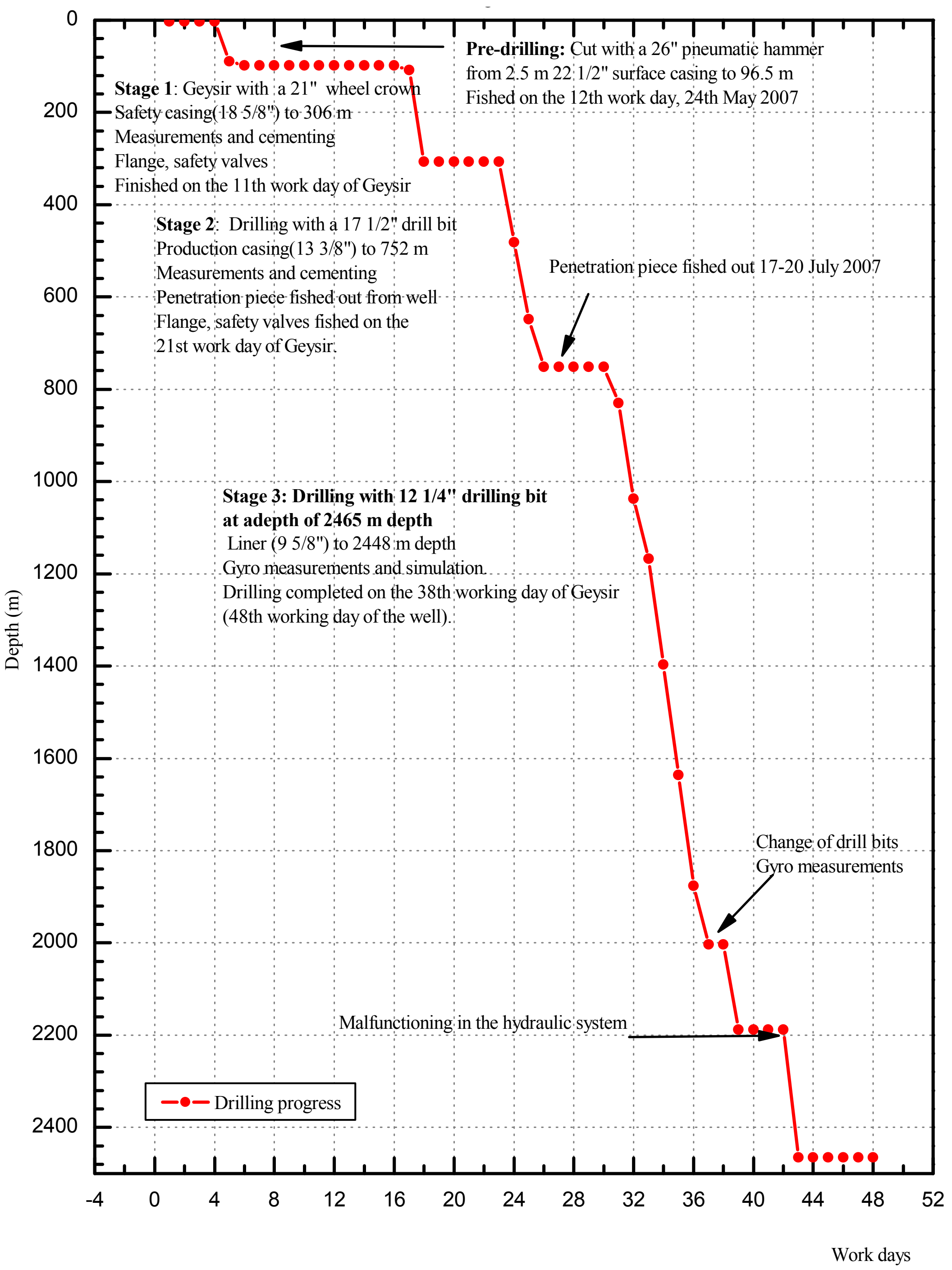

FIGURE 9: Drilling progress of well HE-32

3.3 Stratigraphy

Figure 10 shows the litho-stratigraphy of well HE-32 along with various geophysical logs. The rock formations are mainly hyaloclastites, composed of tuff (basaltic and reworked), basaltic breccia and pillow (glassy) basalts. Fine- to medium-grained basalts (interglacial lava series) form thin layers in between these hyaloclastites at different depths. Two intrusions between 540-546 and 580-596 m were identified together with possible intrusions at various depths of the well; these were mapped but the main concentration was between 656-740 m. The following description of the rock formation is based on binocular observations aided by petrographic thin sections, XRD analysis and geophysical logs. Results of petrographic analysis and X-ray analyses are attached as Appendix II.

No cuttings. (0-4 m)

Basaltic tuff (4-6 m): Mixture of light green fine-grained basalt with vesicular glass, weakly oxidized ground mass with *calcite* as the alteration mineral.

Fine- to medium-grained basalt (6-10 m): Fine- to medium-grained basalt, non-porous, lots of small plagioclase, very fine opaques minerals, probably magnetite and occasionally fresh olivine. Formation is probably a lava flow.

Basaltic breccia (10-20 m): Medium-grained basaltic breccia, vesicularity indicating a porous nature with almost equal proportions of plagioclase and opaque minerals (magnetite-ilmenite). Olivine more visible than in the preceding cuttings and few fresh glassy materials are also present.

Glassy (pillow) basalt (20-58 m): Dark grey to blackish fine-grained basalt, seemingly fresh and with vesicles indicating relative porosity. This has a predominantly crystalline composition with apparent plagioclase and opaques, most likely magnetite or ilmenite. Olivine is common and fresh glassy material increases. *Smectite* was identified in thin section at 30 m. *Calcite* and *limonite* occur as the alteration minerals.

Basaltic breccia (58-62 m): Fine- to medium-grained basalt. Formation is non-porous, almost equal amounts of felsic minerals, predominantly of plagioclase and mafic minerals, probably magnetite. Lots of fresh glass is present. *Calcite* and *limonite* are the alteration minerals.

Glassy (pillow) basalt (62-92 m): Dark grey to blackish fine-grained basalt. Yellowish brown colour is attributed to weathering glass, few phenocrysts of fine- to medium-grained plagioclase tinted with reddish brown limonite. Small olivine crystals yellowish green in colour also are present. Formation is generally porous with some vugs filled with calcite. This rock appears unconsolidated with individual fragments sub-rounded to sub-angular in shape. Alteration minerals are mainly calcium down to 86 m, then a little clay, also identified as *smectite* in thin section between 82-88 m which then increases thereafter. This correspondingly changes the colour of this formation from yellowish to green grey.

No cuttings (92-94 m)

Reworked tuff (94-96 m): Dark green sub rounded to sub angular fine-grained tuffaceous sediments. The tuff is seemingly altered and accordingly soft. It is occasionally tinted with reddish brown mineral, possibly limonite. Fine grains of plagioclase and olivine present, although not common. Fine grains of opaque minerals (magnetite or ilmenite) and glass material present. Other minerals present are *calcite* and *clay*.

No cuttings (96-104 m)

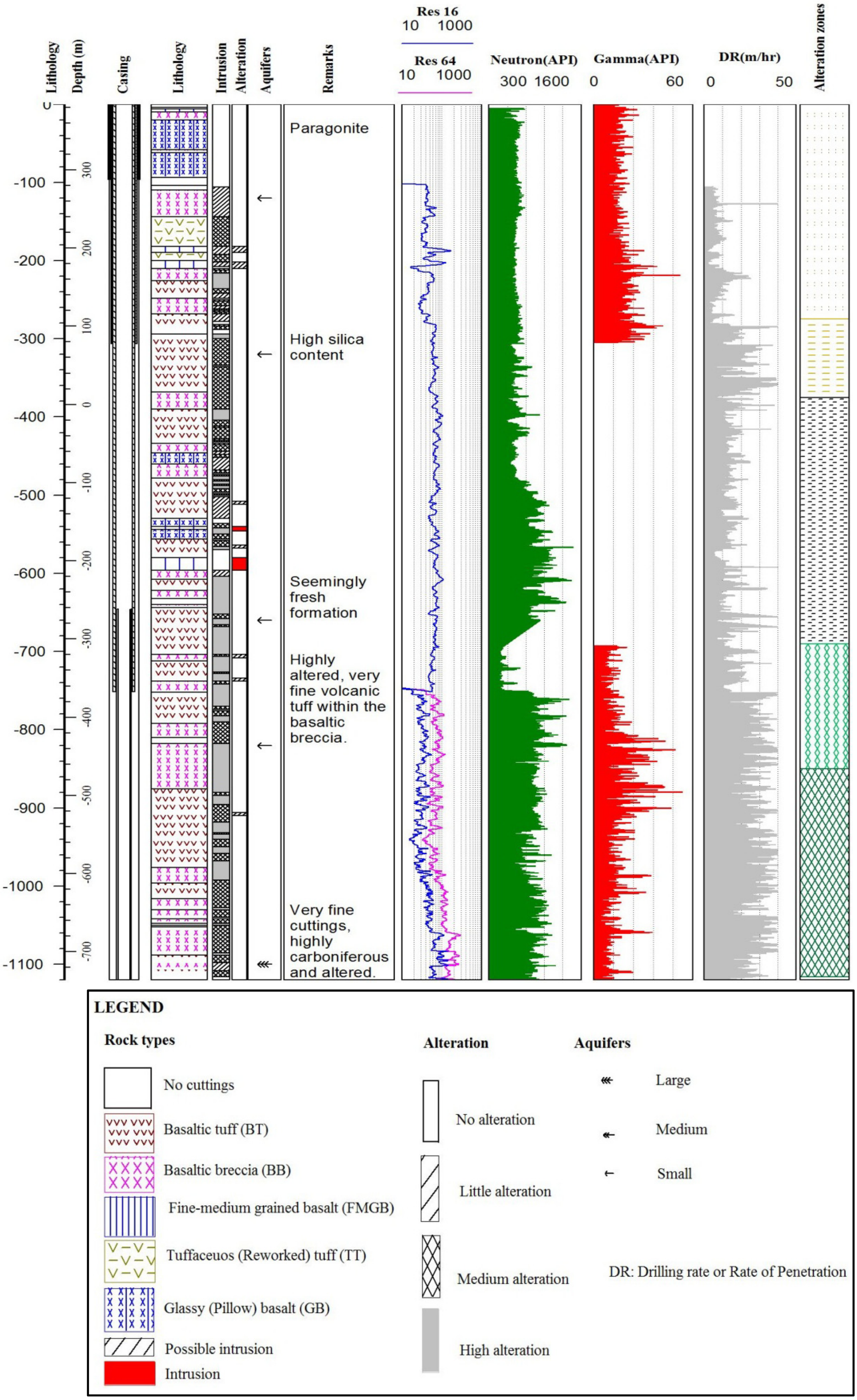

FIGURE 10: Stratigraphic column of the upper 1120 m for well HE-32 together with some of the corresponding geophysical logs

Basaltic tuff (104-110 m): Dark green in colour. Fragments of this basalt are occasionally tinted with reddish brown mineral, possibly limonite. Plagioclase occurs, as does olivine in small quantities. Few fine opaques of probably magnetite or ilmenite are also present as are glassy materials. Alteration minerals are *limonite, calcite and smectite.* The latter was confirmed in XRD-analysis at 106 m.

Basaltic breccia (110-144 m): Dark grey-greenish fragments of medium-grained basalt breccia with a few phenocrysts of plagioclase with small calcite veins. Olivine is also present, though in smaller quantities. Dark grey to greenish clays fill some of the pores and limonite occurs as reddish brown tints on the basalt breccia fragments. Small amounts of *pyrite* and *calcite* are present.

Reworked tuff (tuffaceous sediments) (144-182 m): Mixture of predominantly light grey fragments of volcanic tuff with unconsolidated whitish siliceous sediments, lots of vein fillings with calcite. Dark blue particles in a pore space at 150 m were interpreted as multi-colour *chalcedony*. *Limonite* and *pyrite* also are present, the latter occurring intermittently for example between 162 and 168, at 174 and at 180 m. A rock material white in colour, with neither a clear crystal system nor a clear surface occurs at 166 m. It is non-reactive to dilute hydrochloric acid; it could be either quartz or a zeolite of yet unknown type but possibly *chabazite, analcime or laumontite. Smectite was* detected in both XRD and thin section analyses carried out between 150-182 m.

Fine- to medium-grained basalt (182-190 m): Fine-grained basalt (tholeiitic), dark grey in colour with a few opaque minerals. Calcite and pyrite occur as micro vein fillings, limonite is also present as coatings to the basalt. Another alteration mineral, very fine-grained greyish green clays, fills some pores of this formation. Note a radiating whitish zeolite at 182 m which could not be identified with certainty due to its lack of clear crystal form and faces. It is probably *scolecite or mesolite.*

Reworked tuff (tuffaceous sediments) (190-200 m): Mixture of predominantly greyish to dark grey sediments which are obviously of different origins and seem to have travelled a reasonable distance due to their sub rounded to sub angular shape. A seemingly fresh fragment of greyish and lineated fine-grained tholeiitic basalt is seen which appears to be a dyke. *Calcite* is the common alteration mineral. Pyrite was only observed at 198 m while a reddish fine-grained variety of oxidized clay, probably smectite, appears at 200 m. *Smectite* was confirmed at 196 m in XRD analyses. The porosity of this formation increases with depth.

Fine- to medium-grained basalt (200-210 m): Dark grey fine-grained, tholeiitic basalt with few micro phenocrysts of plagioclase. A few clear olivine crystals are visible which give an indication that the rock is fresh. Light grey to whitish tuffaceous and calcareous formations are there, although in small quantities, between 208-210 m. Pyrite and calcite are the observed alteration minerals. Additionally, smectite was observed in thin section at 202 m.

Basaltic breccia (210-226 m): Mixture of fine-grained (tholeiitic) basalt with whitish to light greyish tuffaceous material of sub-rounded to sub angular shape. Clay, pyrite and calcite are the other alteration minerals present. Smectite, coarse and fine-grained clay, chabazite, chalcedony and opal were identified in thin section at 216 m.

Basaltic tuff (226-248 m): Predominantly light greyish to greenish, tuffaceous and silicic material, sub-rounded to sub angular in shape, highly altered. The light colour may imply richness in zeolites but they are too small to be identified. An alternate name might be acidic tuff due to the seemingly high silica content which was even detected in the high gamma ray count (Figure 10) and can be supported by chemical analysis. Large amounts of clay and pyrite but relatively few amounts of calcite.

Basaltic breccia (248-268 m): Dark grey sub-angular fragments of fine-grained breccia with scattered opaque mineral (magnetite or ilmenite) phenocrysts. Calcite occurs as micro veins whereas clays fill vugs. Quartz occurs between 250 and 252 m and at 260 m. *Analcime* was observed at 254 m. In addition, smectite was identified by XRD analysis at 250 m.

Basaltic tuff (268-288 m): Mixture of predominantly purplish grey, fine-grained and hard basalt with fine-grained dark grey soft tuff sediments. It is a highly porous material with lots of pyrite and is fairly carbonaceous. Clays appear as very fine green to greyish purple grains. Quartz, calcite and clays are the alteration minerals observed.

No cuttings (288-294 m)

Basaltic tuff (294-368 m): Light grey to greenish grey, highly vesicular (thus inferred porous) mixture of predominantly fine-grained and crystalline basalt with fine-grained tuff sediments. It has lots of pyrite and smectite. A radiating, whitish, with flattened and elongated group of crystal fillings, amygdule at 298 m was interpreted to be *scolecite, laumontite or mordenite*. Calcites, clay, amygdales of chalcedony (316 m), and stilbite (330 m) are other alteration minerals observed. High neutron counts infer reduced porosity, probably due to alteration minerals filling the pores. XRD analysis revealed a mixed-layer clay zone between 300-350 m. *Note:* It may be a thick tephra (sub aerial) formation, highly silicic in composition. Detailed chemical analysis, for example ICP, is proposed for further classification and subdivision of this formation.

Basaltic breccia (368-390 m): Dark grey, fine-grained basalt with numerous vugs, some occupied by calcite. Vein calcite also occurs as does quartz, though in small quantities. In some places the latter is in amygdales and surrounded by the former. Green colour is probably due to clays (smectite). A whitish mineral with neither clear crystal faces nor crystal system, probably *wairakite,* was observed at 388 m. Opaque minerals (magnetite-ilmenite) within a greenish grey tuffaceous highly altered matrix are also present. Alteration minerals observed at this depth interval are: calcite, pyrite, clay, *thomsonite* (370 m) and *quartz*.

Basaltic tuff (390-434 m): Greenish grey, highly porous, altered and carbonaceous fine-grained basaltic tuff with micro veins of calcite, lots of pyrite and tints of limonite. Platy calcite is also present at times surrounding quartz in both fragments and in amygdales and, in some cases, filling vugs. Opaque minerals occurring as phenocrysts in basalt fragments may be of magnetite or ilmenite. Greenish grey clays fill pores in the tuff formation. Reddish brown tints which can be interpreted as limonite at 388 m were considered to be a rusting material from either the casing or drill string. Thin section analysis at 416 m identified chabazite, mixed-layer clay and wairakite.

Basaltic breccia (434-446 m): Greenish grey, fine-grained and pyrite rich formation. It is massive with a few opaque minerals (magnetite-ilmenite), calcite amygdales and is seemingly siliceous.

Basaltic tuff (446-460 m): Tuff rich basalt, light grey to green in colour and fine grained. It is highly carboniferous, mainly in pores, some of which are filled with opaque minerals. Calcite, pyrite, and quartz are the secondary minerals observed.

Basaltic breccia (460-478 m): Greenish grey to light grey, fine-grained and hard basalt. It is relatively porous with pores filled with calcite and opaque minerals, although few in numbers. Calcite also occurs as micro veins. It appears less silicic than the proceeding formation. Pyrite is also common. The greenish colour is attributed to smectite.

Basaltic tuff (478-530 m): Dark-grey angular to sub-angular, fine-grained fragments of basalts with opaque mineral (magnetite-ilmenite) phenocrysts. It is hard material seemingly fresh with a ground mass of silica, light grey to greenish pyrite rich tuff. Calcite, clay and tints of limonite are the observed secondary minerals. From 500 m onwards, the formation remains the same but with less or no ground mass of smaller fragments. Pyrite occurs both as micro veins and as coatings on mainly tuff material. Clay and calcite are the secondary minerals. Wairakite and quartz are present from 522-

530 m. Mica at 506 m was taken to be alien from the drilling operations. Smectite, a mixed-layer clay and mordenite were observed in a thin section at 508 m while chlorite (unstable) was detected at 500 and 520 m by XRD analysis.

Glassy basalt (530-540 m): Predominantly dark grey, fine- to medium-grained, seemingly fresh, glassy and basaltic rock with whitish precipitates of calcite. Quartz and plagioclase are present, the latter appearing as phenocrysts. Few light grey volcanic tuffs with relatively high content of pyrite also occur. Pyrite also appears as micro veins in the basalt.

Fine- to medium-grained basalt (540-544 m): Light grey-greenish, fine- to medium-grained crystalline basalt, occasionally carrying opaque minerals (magnetite or ilmenite). It appears fresh and with few plagioclase phenocrysts. Calcite, limonite and pyrite are the secondary minerals observed. Calcite and pyrite were confirmed in thin analysis at 540 m, also detecting wairakite and mixed-layer clay.

Glassy basalt (544-556 m): Dark grey-greenish, fine-grained glassy and basaltic rock, seemingly fresh with a few olivine crystals discernable. Dark inclusions spread almost throughout this formation, probably of opaque minerals of either magnetite or ilmenite. Calcite occurs as both platy grains and as veins. Pyrite occurs in small quantities. Greenish grains of clay occupy some voids in the basalt. *Wairakite* was also observed at this depth. XRD analysis detected chlorite (unstable) at 550 m.

Basaltic tuff (556-580 m): Mixture of fine- to medium-grained, dark grey basalt with light grey to green very fine grey volcanic tuff. This formation is relatively rich in pyrite both as micro veins and as yellowish brown tints on this formation. Quartz crystals are evident, although not common. It is weakly to moderately altered, the greenish colour attributed to a clay mineral variety, smectite. Calcite is also present and *wairakite* was only observed at 560 m depth. The occurrence of wairakite was also revealed by a thin section analysed at 564 m which additionally detected quartz and mixed-layer clay. Opaque minerals, probably magnetite or ilmenite, occur as dark spots within the voids of the basalt formation. Fresh glassy material, especially at 568 m, was interpreted to be a dyke cutting through this formation. XRD analysis further detected chlorite (unstable) at 570 m.

Fine- to medium-grained basalt (580-596 m): Dark grey-light grey, fine- to medium-grained basalt. Opaque minerals (magnetite-ilmenite) appear as dark spots within this seemingly fresh formation. Calcite occurs both as white precipitates and void fillings. Other secondary minerals observed are clays.

Porphyritic basaltic breccia (596-608 m): Dark grey-greenish, fine- to medium-grained crystalline rock with minor light grey to greenish tuff. It is of two types: weakly and moderately altered. Calcite and *quartz* veins are seen in this formation, while pyrite, mostly in micro veins, is also present though in small quantities.

Basaltic tuff (608-622 m): A composite of grey-greenish, fine- to medium-grained, porphyritic breccia and light grey, very fine-grained volcanic tuff. Opaque minerals (magnetite or ilmenite) occur as dark patches uniformly distributed within the basalt whereas pyrite appears as yellowish tints on the basalt fragments and is more widely distributed in the volcanic tuff. Platy calcite is common as are clays. The first appearance of chlorite was confirmed at 600 m through XRD analysis.

Basaltic breccia (622-632 m): Mixture of dark grey-greenish, weakly altered and light grey moderately altered fine- to medium-grained basaltic breccia. Opaque minerals (magnetite or ilmenite) occur as dark patches uniformly distributed within this formation. Pyrite is apparent, especially the light grey variety. Few volcanic tuffs, whitish in colour and fine grained, are present. Calcite fills most of the voids. Clay minerals are also evident in binocular microscope, which were confirmed as chlorite at 620 m by XRD analysis.

Basaltic tuff (632-640 m): Predominantly light grey, fine-grained volcanic tuff and minor dark grey, fine- to medium-grained basalt. *Prehnite, wairakite*, pyrite, calcite and clays are the secondary minerals observed. Mixed-layer clay and chlorite were observed in thin section at 634 m.

Basaltic breccia (640-644 m): Light grey-greenish volcanic tuff which is rich in basaltic breccia. Opaque minerals (magnetite or ilmenite) appear as dark spots, especially in the basaltic breccia. Pyrite, calcite, feldspar (likely adularia) and quartz are observed. Coarse feathery clay (chlorite) is another alteration mineral present.

Basaltic tuff (644-704 m): A multiple of grey-greenish, fine- to medium-grained, porphyritic breccia and light grey very fine-grained volcanic tuff. It is a highly altered formation with a little fresh glass material. Opaque minerals (magnetite or ilmenite) occur as dark patches uniformly distributed within the basalt. Alteration minerals present are: siderite, pyrite, calcite, clay, prehnite, laumontite and epidote. Mixed-layer clay and chlorite were identified in thin section at 662 m while laumontite was detected by XRD analysis, and at 600 and 620 m.

Basaltic breccia (704-712 m): Light grey-greenish volcanic tuff which is rich in basaltic breccia. Opaque minerals (magnetite or ilmenite) appear as dark spots, especially in the basaltic breccia. Pyrite, calcite, epidote, clay and laumontite are observed. Petrographic analysis of a thin section at 706 m also identified laumontite in addition to the occurrence of other high-temperature minerals like quartz, prehnite and chlorite.

Basaltic tuff (712-738 m): A combination of grey-greenish, fine- to medium-grained, porphyritic breccia and light grey very fine-grained volcanic tuff. It is a highly altered formation. Opaque minerals (magnetite or ilmenite) occur as dark patches uniformly distributed within the basalt. Mafic consolidated and crystalline rock fragments between 728-738 m were interpreted as an intrusion. Alteration minerals present are: a large amount of prehnite and wairakite, siderite, pyrite, calcite, clay and epidote. Chlorite was the only clay mineral identified by XRD analysis at both 700 and 720 m while albite, quartz, laumontite and also chlorite were identified in thin section analysis at 734 m.

Basaltic breccia (738-752 m): Dark-grey to light grey-greenish, fine-grained basaltic breccia. Calcite, pyrite, fine-feathered clay and prehnite are present.

Basaltic tuff (752-792 m): A complex of grey-greenish, fine- to medium-grained, porphyritic breccia and light grey very fine-grained volcanic tuff. It is a highly altered formation. Opaque minerals (magnetite or ilmenite) occur as dark patches uniformly distributed within the basalt. Alteration minerals present are: clay, prehnite, pyrite, quartz and calcite.

Basaltic breccia (792-810 m): Dark grey to light grey-greenish fine-grained basaltic breccia with mafic crystalline rocks, assumed to be an intrusion. Calcite, pyrite, fine feathered clay and prehnite are present. Chlorite was detected at 800 m by XRD analysis.

Basaltic tuff (810-818 m): Mixture of dark grey to light grey, fine- to medium-grained basalts carrying patches of opaque minerals (magnetite or ilmenite) with relatively few purplish grey volcanic tuff. Prehnite, quartz, fine feathered clay and pyrite are present.

Basaltic breccia (818-876 m): Dark grey-greenish and whitish basaltic breccia, highly carbonaceous and altered. Opaque minerals of probable magnetite or ilmenite, or both, are evident. Quartz, wairakite, pyrite, limonite, clays and calcite are also present. Chlorite too, was detected by XRD analysis at both 800 and 850 m depth, which also revealed the probable first occurrence of amphibole, most likely actinolite.

Basaltic tuff (876-976 m): Predominantly light grey-greenish, fine-grained volcanic tuff and little dark grey, fine- to medium-grained basalt. It has relatively high levels of opaque minerals. *Quartz,* *epidote, prehnite, wairakite*, pyrite, calcite and clays are common secondary minerals observed. It is worth noting that boundaries of different sections within this formation are not well defined. We have attempted to sub-divide it into 6 different units, using detailed geophysical logs (Section 3.5.4). Quartz and epidote were also confirmed in a thin section analysis at 906 m which also showed the existence of albite and chlorite. The latter was also analysed by XRD analysis of samples at 900 and 950 m.

Basaltic breccia (976-996 m): Dark grey-greenish and whitish basaltic breccia, highly carbonaceous and altered. Opaque minerals of probably magnetite or ilmenite, or both, are evident. Quartz, wairakite, pyrite, clays and calcite are the observed secondary minerals.

Basaltic tuff (996-1016 m): Mostly light grey-greenish, fine-grained volcanic tuff and little dark grey, fine- to medium-grained basalt, with relatively high levels of opaque minerals. *Quartz, epidote, prehnite, wairakite*, pyrite, calcite and clays are common secondary minerals. Amphibole, most likely actinolite, was detected at 1000 m by XRD analysis.

Basaltic breccia (1016-1028 m): Dark grey greenish and whitish basaltic breccia, highly carbonaceous and altered. Opaque minerals of probable magnetite or ilmenite, or both, are evident. Quartz, wairakite, pyrite, clays and calcite are the observed secondary minerals.

Loss of circulation (1028-1030 m)

Basaltic breccia (1030-1040 m): Dark grey-greenish and whitish basaltic breccia, highly carbonaceous and altered. Opaque minerals of probable magnetite or ilmenite, or both, are evident. Quartz, wairakite, pyrite, clays and calcite are the observed secondary minerals.

No cuttings (1040-1042 m)

Basaltic breccia (1042-1048 m): Dark grey-greenish and whitish basaltic breccia, highly carbonaceous and altered. Opaque minerals of probable magnetite or ilmenite, or both, are evident. Quartz, epidote, pyrite, clays and calcite are the observed secondary minerals.

Reworked tuff (1048-1050 m): Greyish-green, fine- to medium-grained, highly altered and carbonaceous tuffaceous sediments. Clay, calcite, quartz, and epidote are the alteration minerals visible.

Basaltic breccia (1050-1052 m): Dark grey-greenish and whitish basaltic breccia, highly carbonaceous and altered. Opaque minerals of probable magnetite or ilmenite, or both, are evident. Observed alteration minerals are: quartz, epidote, pyrite, clays and calcite.

Reworked tuff (1052-1056 m): Greyish-green, fine- to medium-grained, highly altered and carbonaceous tuffaceous sediments. Alteration minerals visible are: clay, calcite, quartz and epidote.

Basaltic breccia (1056-1086 m): Dark grey-greenish and whitish basaltic breccia, highly carbonaceous and altered. Opaque minerals of probable magnetite or ilmenite, or both, are evident. Observed alteration minerals are: quartz, epidote, pyrite, clays and calcite. A rare occurrence of *garnet* was observed at 1084 m depth. Quartz and epidote were also detected in thin section at 1064 m and also albite and quartz at the same depth.

Loss of circulation / no cuttings (1086-1088 m)

Basaltic tuff (1088-1098 m): Primarily light grey-greenish, fine- to medium-grained volcanic tuff with relatively little amounts of dark grey, fine- to medium-grained basalt. It has moderately high levels of opaque minerals. *Quartz, epidote, prehnite, wairakite*, *wollastonite*, pyrite, calcite and clays are common secondary minerals observed, apart from wollastonite; the before-mentioned alteration minerals were also identified in thin section analysis at 1074 m.

Basaltic breccia (1098-1106 m): Light grey to greenish, fine- to medium-grained basalt, seemingly fresh with minute amounts of purplish brown volcanic tuff. *Quartz, epidote, prehnite, wairakite*, *wollastonite*, pyrite, calcite and clays are the common secondary minerals observed. It is of interest to note that wollastonite was also detected in thin section at 1100 m, occurring together with chlorite and the aforementioned minerals.

Basaltic tuff (1106-1116 m): Mixture of almost equal amounts of grey-greenish, fine- to medium-grained basalt and purplish brown fine-grained volcanic tuff. Opaque minerals of either magnetite or ilmenite, or both, are present although in small amounts, as is whitish calcite. Secondary minerals present are: *quartz, epidote, prehnite, wairakite*, *wollastonite*, pyrite, calcite and clays.

Total loss of circulation / no cuttings (1116-2465 m)

3.4 Intrusions

By definition, an intrusion is an emplacement of magma into pre-existing rock. As such, they usually show relatively coarser textures compared to the host rock since the subterranean magma cools slowly giving time for crystal growth. However, they may be fine-grained or aphyric when the intrusions/dykes consolidate at shallow depths and/or if they are small (thin). Moreover, they show oxidation where heating effects have been prominent along their boundaries (e.g. Gebrehiwot, 2010). Furthermore, the rocks are identified by their massive, tight or compact nature and appear fresh in comparison to the surrounding lithology.

A couple of intrusions were mapped in well HE-32, one between 540-546 m, and a second one between 580-596 m. Additionally, several probable intrusions were identified at different depth intervals for example 182-190, 202-208, 564-568 and 734-736 m. They are fine- to medium-grained rocks. They show elevated peaks in the geophysical logs, especially in the neutron and resistivity logs with a reduced rate of penetration or drilling rate (Figure 10). By binocular microscopy, intrusive rocks were characterised by a dark grey colour, no vesicles and appeared shiny and generally fresher than other cuttings. Optical microscopy revealed that the main mineralogical assemblages in these intrusive rocks are: phenocrysts of plagioclase, olivine and pyroxene; the texture is porphyritic.

A comparison made with neighbouring wells HE-3 and HE-51 separated respectively by ~5 and 100 m indicates that intrusions occur almost at the same level at about 200 m and between 500-600 m in all three wells, but between 800-900 m in well HE-51 and HE-32. Details are described in Section 5.

3.5 Geophysical logs

During drilling the on-site borehole geologist constructs a lithological column based on cuttings obtained at constant depth intervals of, normally, 2 metres. The rate of penetration is, however, usually very high and, therefore, the constructed lithological logs have a lower resolution than could be obtained under usual conditions or through drill cores. Additionally, cuttings analysis suffers several limitations that do not affect geophysical logs. These include the following (e.g. Browne, 1978; Mostaghel, 1999; Low, 1977):

Depth shift: Cuttings are carried to the surface by the drilling fluid. When a sample of cuttings is sampled at the surface, it is labelled with the drilling depth at the time the sample was taken. However, the real depth where the cuttings originate from is decreased by the number of metres that were drilled during its travel to the surface. The effect of the time delay is to shift the depth readings of the cuttings downward, relative to the logs; i.e. a lithological boundary observed in the cuttings appears to be located at a greater depth than the true depth. The size of the shift depends on: well diameter, type of drilling fluid, pumping rate, and circulation loss and drilling rate. Delay times are much greater when the drilling fluid used is water than when mud is used. The onsite borehole geologist, using a formula which takes into account all the above factors, corrects the depth readings of the cuttings samples. However, the factors are not always accurately known, so there is a limit to the accuracy of this method. Furthermore, there is always the possibility of some error affecting the depth readings, due to the many manual steps involved.

Smearing-out of lithology: Cuttings of different size travel to the surface at different speeds. This leads to a separation of the cuttings according to size during upward transport and a smearing-out of the cuttings record occurs. The presence of large cavities in the well also leads to a decrease in the resolution of the cuttings record, because local circulation of drilling fluid within the cavity leads to a mixing of cuttings from different depths. High and variable drilling rates also contribute to this effect as do low flow rates of returning drilling fluid caused by large circulation losses. The smearing-out effect reduces the resolving power of the cuttings record, i.e. the possibility of identifying thin layers and the accuracy with which the depth and thickness of stratigraphical boundaries can be determined.

Misidentification of lithology: When the drill bit grinds the cuttings too finely, accurate identification of lithology may become very difficult using standard methods of cuttings analysis. Loss of resolving power due to the smearing-out effect may make this even harder. Drilling with a mud motor often causes the cuttings to be ground to such a small size that interpretation of the lithology becomes very difficult.

Intermittent or total loss of circulation, meaning cuttings are not obtained as often as required or not obtained at all for quite a long depth interval. The latter situation becomes more significant when it happens in the perforated casings (liner) part where nature and competence of the rock types are of most importance for the future operations, for example, to avoid collapsing or loose material which may cause silting. The geophysical logs are, therefore, used to improve the interpretation obtained from the cuttings record. It should, however, be emphasized that the analysis of cuttings is the primary source of information which provides the basic litho-stratigraphic framework with which the geophysical logs can be compared and make large improvements in the lithological description. Once the typical log signature of the rock types encountered in the well has been established, deviation from this signature can be used to identify intervals where lithology has been misidentified and even make predictions of the probable lithology where there is loss of circulation.

Well HE-32 presents a typical case where the composition and texture of the lithology are rather uniform; macroscopic and microscopic descriptions have not exhaustively delineated their variation. For instance, the boundaries in the lithology, especially between 800-980 m, are not well defined. Additionally, there was a loss of circulation for a long depth interval, extending in the liner casing portion. We have, therefore, attempted to improve and also propose the lithology in some portions of the well using geophysical logs.

3.5.1 Overview of the geophysical logs used in this study

A number of the geophysical logs were used in this study. These are: nature gamma rays, caliper, neutron-neutron, resistivity and temperature logs; a brief description of each follows.

Natural gamma logs: Different concentrations of radiogenic elements, uranium, thorium, and potassium in various geological formations make it possible to use natural gamma rays (GRL) to map different geological units in wells (Stefansson et al., 1982). In basalts, the natural gamma log is sensitive to several stratigraphic characteristics, the most important of which is anomalous potassium content in basalt and clayey inter-beds (Helm-Clark et al., 2004.). Basalts have very low potassium, uranium and thorium concentrations, where a potassium concentration usually dominates the natural gamma signatures. On the other hand, the clay content of sedimentary inter-beds commonly contains higher levels of potassium, uranium, and/or thorium than the basaltic flows themselves. As such, gamma rays generally show low values in the fresh rocks and a general increase in the alteration zone. In Iceland, GRL have been used for the last 40 years, and in early 1980s an interpretation method was proposed where the GRL could be expressed as the concentration of SiO_2 of the rock (e.g. Stefansson et al., 1982). Gamma logs can therefore reveal the presence of evolved formations.

Neutron logs: The physical basis of measurement of neutron geophysical logs is the scattering and capture of neutrons; the main purpose is to estimate formation porosity (Ásmundsson, 2011). If all of the formation´s hydrogen is contained in the form of liquids, and if these liquids completely occupy the total pore volume, hydrogen richness is an index to porosity (e.g. Njue, 2010). Water saturated basalts (aquifer hosted basalts) show the lowest neutron flux in saturated inter-beds, flow breaks and fracture zones and moderate to high flux in flow interiors (Helm-Clark et al., 2004). For instance, in our analyses (Figure 10), neutron logs revealed reduced neutron flux around 710-760 m; indeed, the aquifer was located around this depth, using drillers log which further supports the fact that the pores within these locations are saturated.

Resistivity logging: The challenge in distinguishing between rock units and their thickness (that is stratigraphic studies) in geothermal wells is often overcome by resistivity logs. Furthermore, it serves as the best method to check the results of surface geo-electrical explorations, specifically TEM (e.g. Ásmundsson, 2011). The underlying principle stems from the definition of resistivity which is basically the inverse of conductivity and the fact that most rock types are resistant to electric currents. On the other hand, water is conductive compared to most earth materials, so when water is present in a rock, it will dominate any resistivity measurements. Assuming that resistivity response is a measure of water content, then resistivity in porous rocks can be treated as a function of water-filled porosity (Helm-Clark et al., 2004). Mostaghel (1999) investigated the behaviour of resistivity logs in igneous rocks in Krafla, Northern Iceland with the result that whereas an igneous rock matrix is generally a poor electrical conductor at geothermal temperatures, the same rock with appreciable porosity or fluid filled vesicles will show somewhat lower resistivity. It is also possible to use resistivity to identify thin zones of increased permeability since permeable zones have higher water content in saturated strata.

Temperature logs: Temperature logging in boreholes provides a wide variety of information, for example, the geothermal gradient and heat flow, the effect of aquifer flow on subsurface temperatures, and the mechanics of fault zones (Helm-Clark et al., 2004). The effects, of a hot or cold flow into or out of the well from the formation, cause a sudden increase or decrease in the temperature, providing important clues to the position of aquifers in the borehole. In the current study, we have limited the use of temperature logs for this purpose.

Caliper logs: Also known as the log of the diameter of the well (e.g. Mostaghel, 1999), caliper logs are important in many aspects in subsurface geothermal evaluation of the borehole, both during and after drilling. These include, but are not limited to: identification of fractures and possible water-producing or receiving zones (where collapsed formations are considered to harbour void spaces), and correction of other geophysical logs for changes in the borehole diameter and others (e.g. Mostaghel, 1999; Senior et al., 2005). In the current investigation, they have been used in the identification of aquifers.

3.5.2 Identification of signatures for the selected geophysical logging method

Correlation between the lithology and geophysical logs for well HE-3 and HE-51 (drilled on the same well pad as well HE-32) was carried out in this study to identify signatures for the geophysical logs in relation to the lithological rock formations encountered (Figure 11 and Table 2). It is interesting to observe that the characteristic signatures so identified for basaltic breccia and fine- to medium-grained basalt are comparable to Mostaghel´s (1999) investigation of the same rock type in Krafla, north Iceland.

TABLE 2: Four signatures identified for the respective rock formations (Scale: 1=low, 2=moderate and 3= high)

Rock unit	Neutron (1-3)	Gamma (1-3)	Resistivity (1-3)	Drilling rate (1-3)	Wells used
Fine- to medium-grained basalt (FMGB)	2	1.5	2.5	1	HE 3 and 51
Basaltic breccia (BB)	1	1	1	2.5	HE 51
Baltic tuff (BT)	2.5	1	2	2	HE 03
Glassy basalt (GB)	1.5	1	2.5	2	HE 03

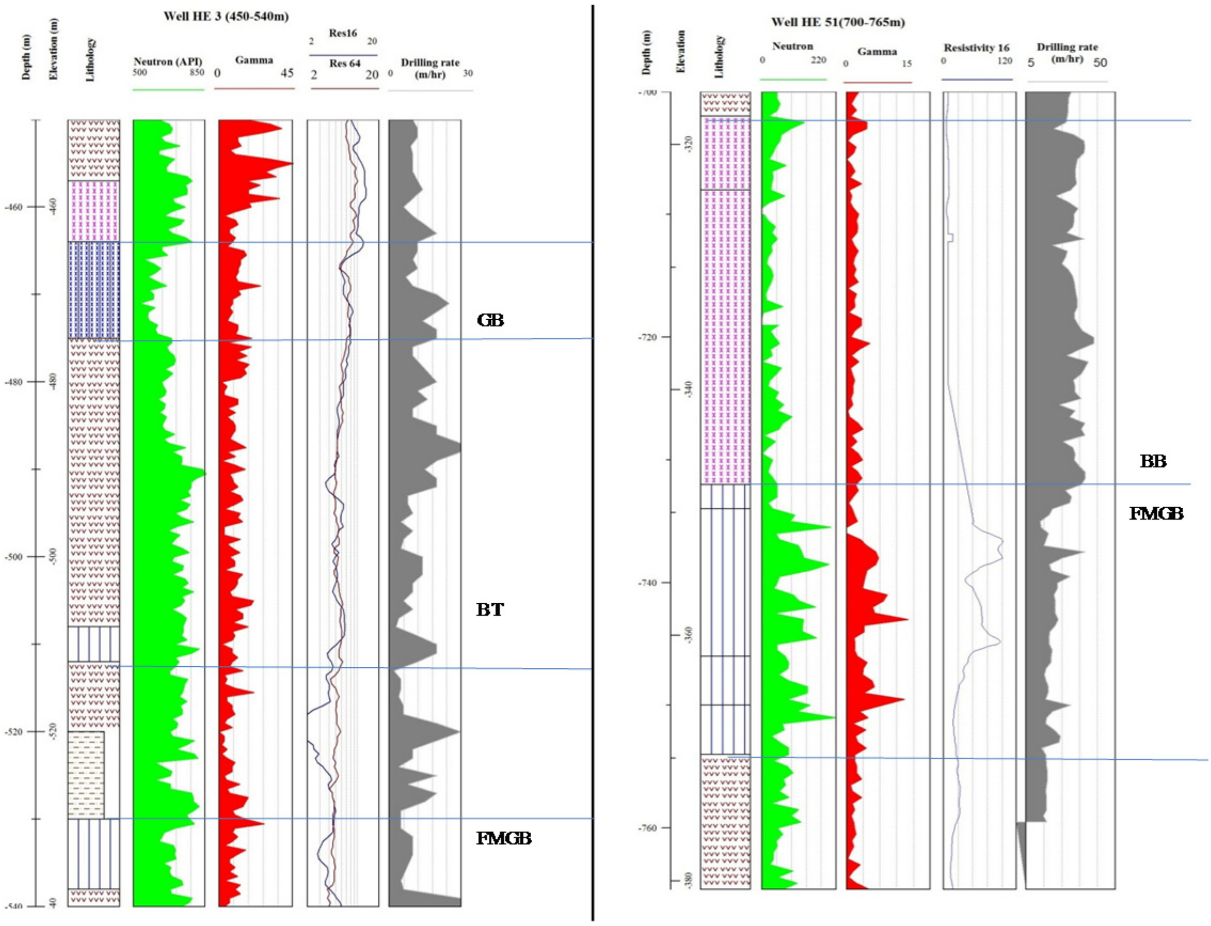

FIGURE 11: Correlation of lithology and geophysical logs in wells HE-3, HE-32 and HE-51; note that the depth is different in the wells; for abbreviations refer to Table 2

3.5.3 Modification of the stratigraphy

Based on the identified signatures for the rock formation (Section 3.5.3), an attempt has been made to modify the lithology of well HE-32, specifically the subdivision of the lithology described as basaltic breccia between 800-900 m (Figure 12), which was difficult to resolve using binocular microscopy. The interpretation of the lithological column was improved and a number of new layers were added:

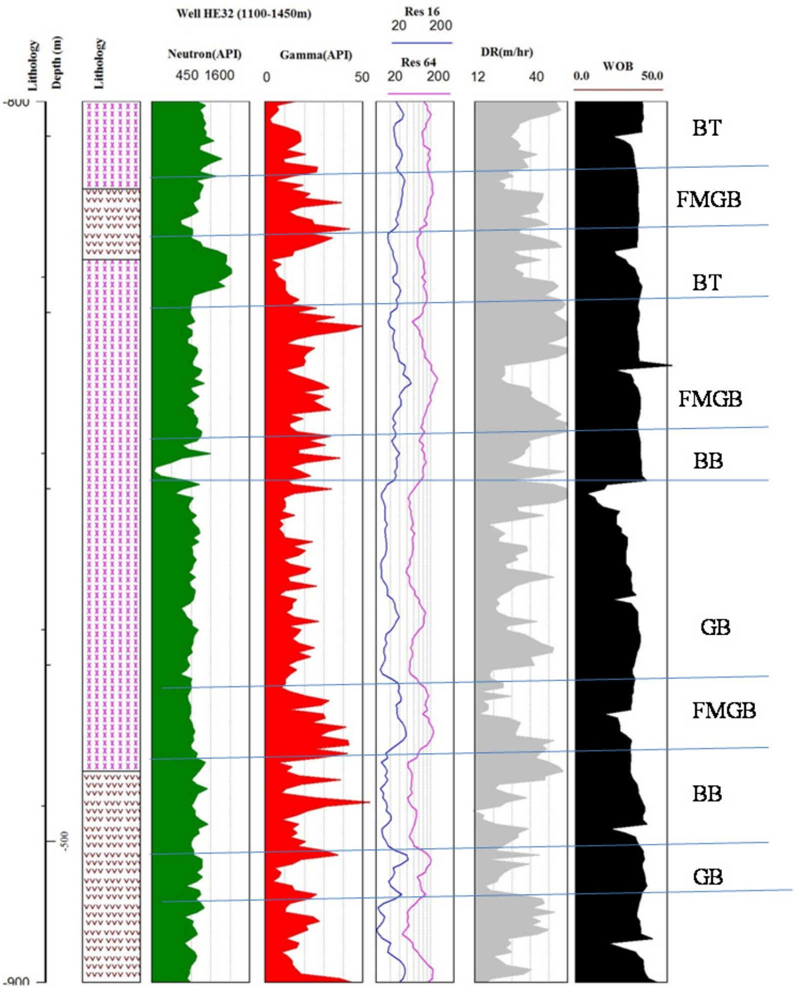

FIGURE 12: Modification of lithology for part of well HE-32 (800-900 m) based on geophysical logs

a) The basaltic breccia between 800-808 m was replaced by basaltic tuff. Moderately high neutron activity and resistivity are the reasons for this substitution.
b) In the same way, basaltic breccia is proposed between 818 and 822 m.
c) At a depth of 808-818 m, a layer of fine- to medium-grained basalt (FMGB) is inferred from the medium neutron activity low- to medium gamma activity, moderate high resistivity and reduced drilling rate while the weight on the bit is relatively high, compared to the basaltic tuff unit interpreted above.
d) For the same reason as above, two FMGB layers interpreted at a depth of 822-838 m and 864-876 m have replaced the breccia layer.
e) Two layers of glassy basalt are proposed between 822-864 and 884-886 m due to low-moderate neutron activity, low gamma ray activity, moderate-high resistivity and a low drilling rate. However, chemical analysis, for example ICP, needs to be carried out to validate these findings.

In a similar way we have predicted the possible lithology in the lower part of the production zone for the interval from 1116 to 1900 m, where cuttings are lacking due to loss of circulation. However, it should be noted that although total loss of circulation was encountered from 1116 to 2465 m, the lack of neutron and gamma logs below 1900 m limited our capacity to predict beyond this depth. A total of 8 boundaries within 4 rock units have been predicted from the logs (Figure 13).

3.6 Aquifers/feed zones in well HE-32

Aquifers are underground layers of water-bearing permeable rock or unconsolidated materials. Generally, the movement of sub-surface water is controlled by the type of rock formations, the characteristics of its permeability and porosity, the temperature and pressure of the sub-surface environment, natural recharge, and the hydraulic gradient (Reyes, 2000). The presence of structural formations such as faults, fractures, joints, and lithological contacts, are positive indications of geothermal feed zones. The identification of strong, good aquifers during or after drilling, or generally prior to well construction is very important for effective extraction of hydrothermal fluids and steam.

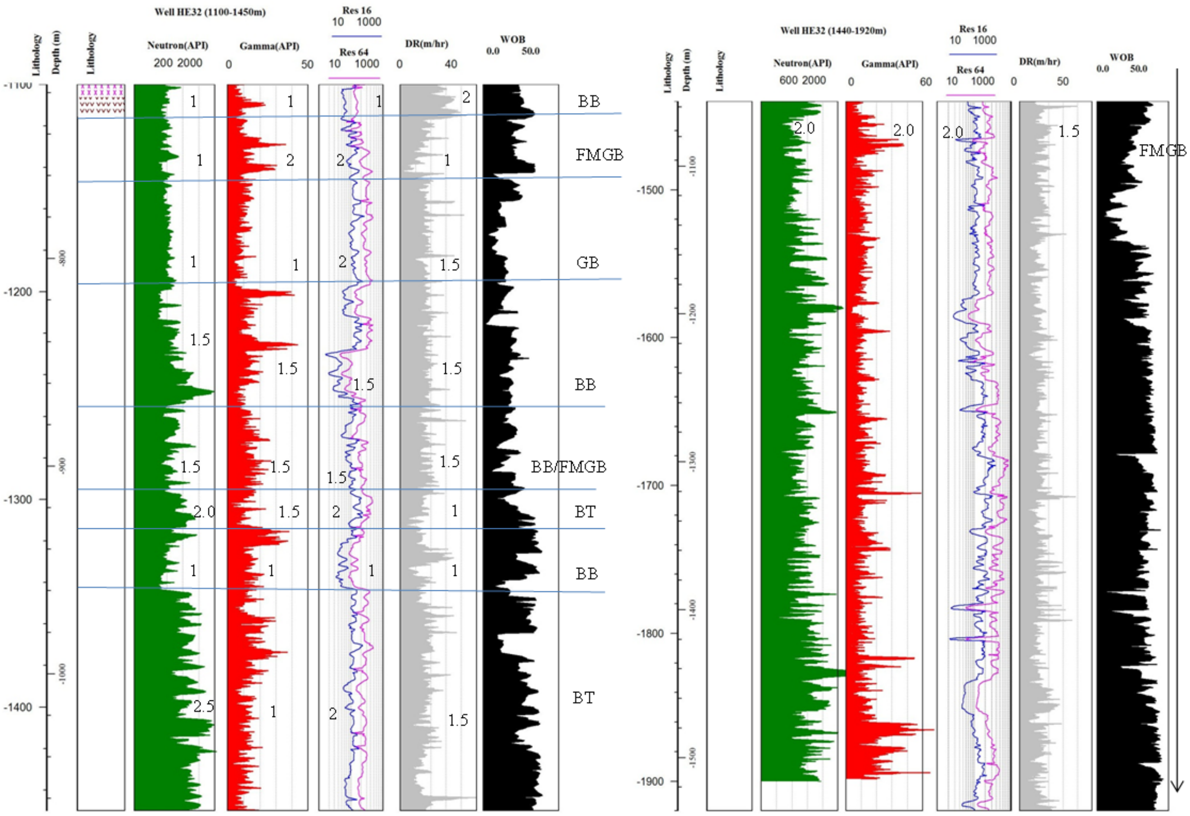

FIGURE 13: Prediction of the lithology in well HE-32 using characteristic signatures of geophysical logs; abbreviations of formations and the scale of numbers used are given in Table 2; and minor variations in geophysical logs are evident beyond 1450 m; it seems to be the same formation, FMGB

Temperature and pressure logs with information on circulation losses/gains during drilling, and alteration and geophysical logs are the main sources for data used to locate aquifers (Franzson, 1998). Caliper or diameter logs are also used in the identification of aquifers. A brief description of both temperature and caliper logs is given, together with the general importance of geophysical logs, in Section 3.5.1. Drilling data, such as the rate of penetration or the pumping rate may also be used. A high rate of penetration during drilling may be an indicator of aquifers, whereas a drop in pipe pressure, especially a total loss of circulation in the zones, may indicate the same (e.g. Koestono, 2007). Examination of rock cuttings is an indirect approach in determining aquifers. The presence of numerous shredded rocks (mylonites), abundant vein networks, and a high concentration of alteration minerals are indications of the presence of strong sub-surface hydrological circulation (e.g. Quintero Roman, 2010). Alteration minerals such as crystallised quartz, adularia, anhydrite, wairakite, illite, hyalophane, abundant pyrite and calcite are also positive signs of good permeability. However, the absence of these alteration minerals, a low degree of alteration, the precipitation of prehnite pumpellyite, pyrrhotite, large quantities of laumontite and titanite (Reyes, 2000) and andesine (Browne, 1978) can be attributed to low-permeability zones.

As noted in Section 3.2, well HE-32 is a directional well connected to fractures and faults in the northeast where some surface manifestations can be found, and cuts through other faults that are located farther south and southeast (Hardarson et al.,2010b; Hardarson et al.,2010c; see also Figure 6). Although the author saw the aforementioned faults in the field, he never observed any signs that well HE-32 had intersected faults using cutting descriptions of binocular microscope results and thin section analysis. While pyrite and calcite appear almost throughout the logged part of the well, euhedral quartz was first seen at 274 m, indicating that it crystallized within larger open spaces. However, the most reliable quartz occurrence is that observed at 522 m where it occurs with the first appearance of wairakite. Other signs of permeability observed along the extent of the well were adularia at 642 m and the all-inclusive degrees of alteration in the well. This is consistent with the observed, though small, positive temperature gradients of all the temperature measurements (Figures 14 and 15).

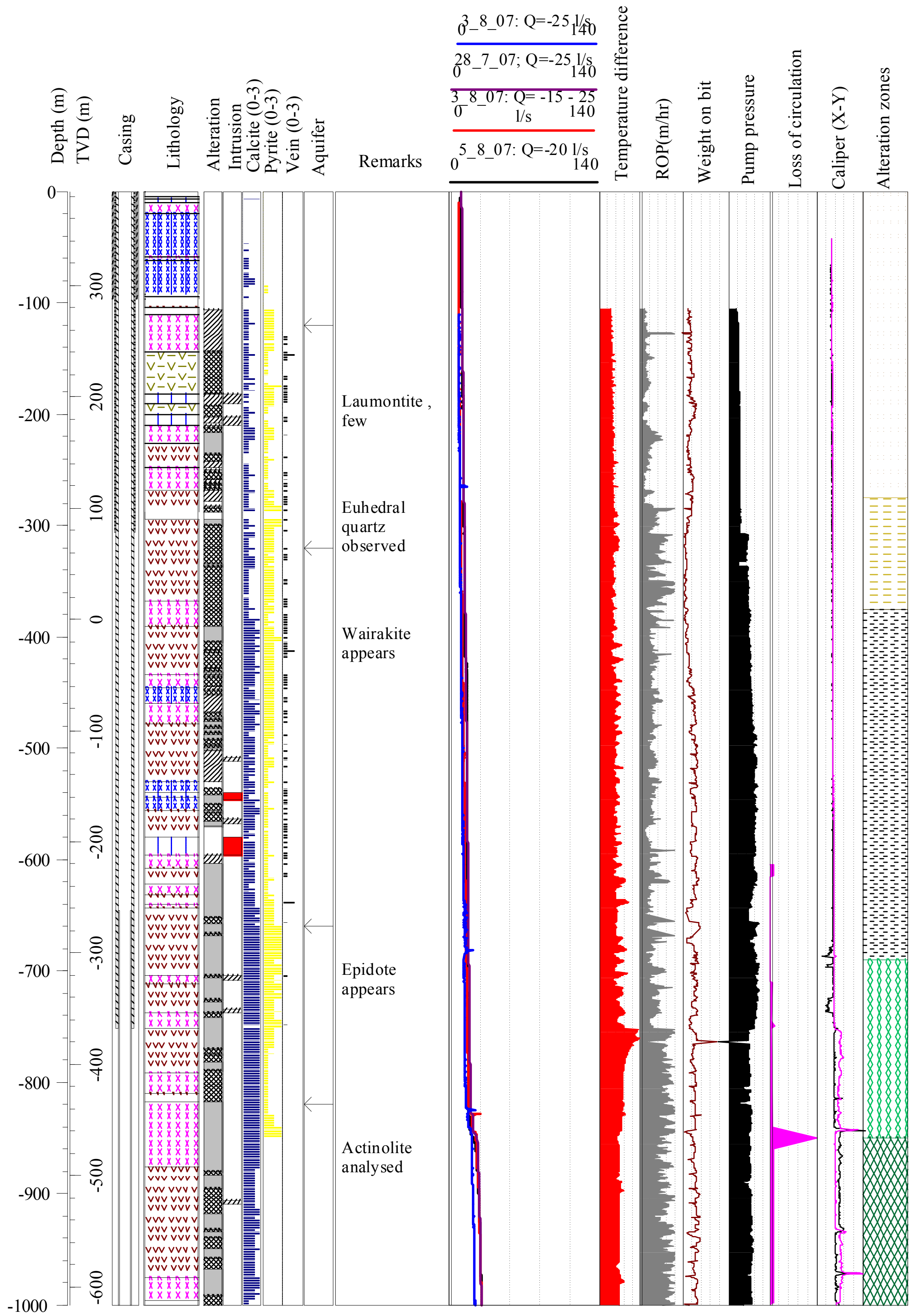

FIGURE 14: Lithology and drillers logs showing the location of aquifers in the upper 1000 m of well HE 32; for legend see Figure 10

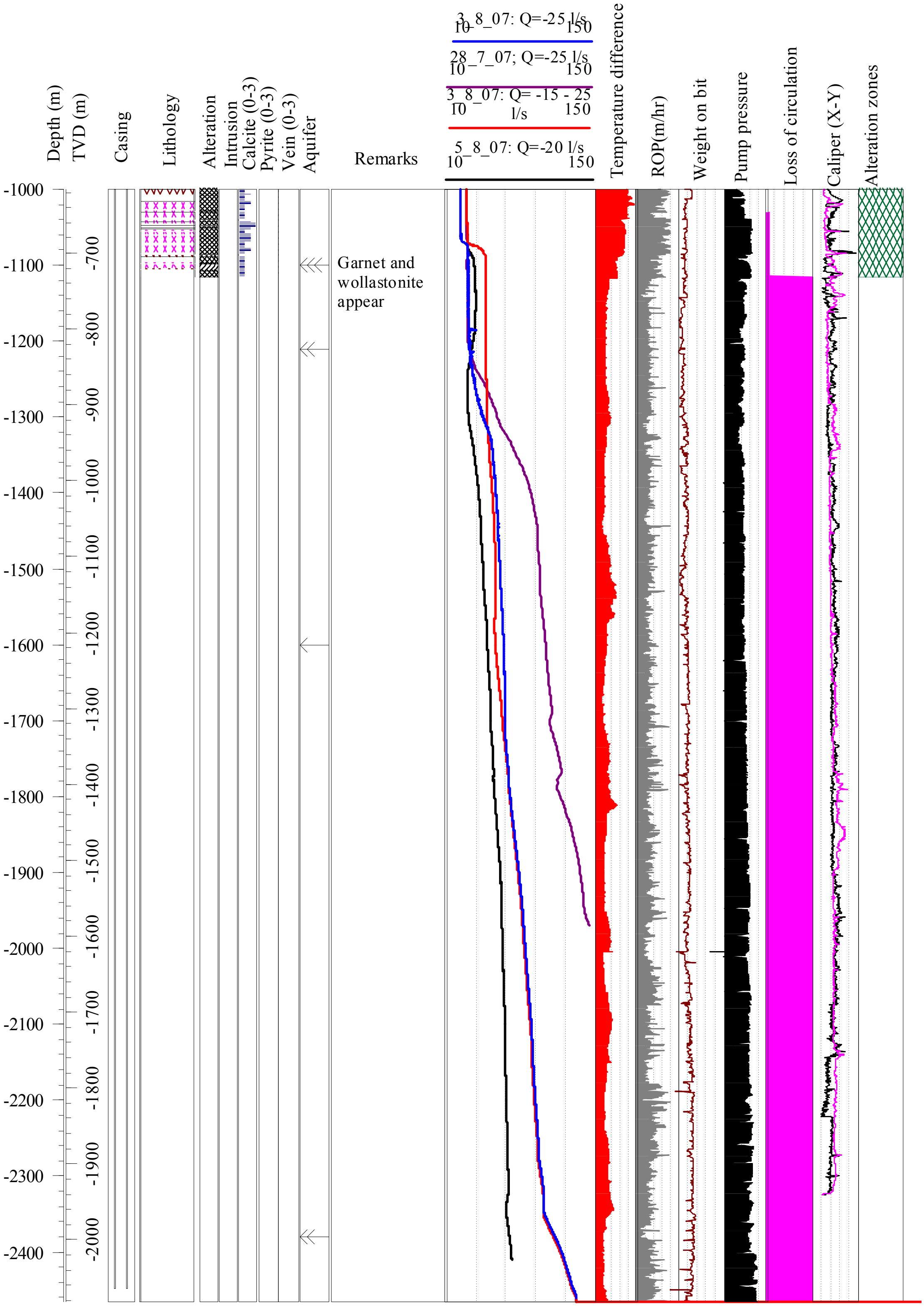

FIGURE 15: Lithology and drillers logs showing the location of aquifers in the lower part of well HE 32; for legend see Figure 10

The location of aquifers/feed zones in well HE-32 (Figures 14 and 15) is aided by relating the sudden increase in the temperature gradients with almost consistent decreased temperature differences, decreased weight on the bit, decreased pump pressure, increased rate of penetration and loss of circulation. Moreover, the diameter (caliper) logs show an abrupt increase in areas around the identified aquifers. When comparing these locations with the lithological description, it is also interesting to note that the identified aquifers in the upper 1100 m could be correlated with nearby lithological contacts. Some relationship between the alteration minerals and permeability was also seen in the well. For instance, there is a high intensity of alteration in association with the aquifer at 840 m and, in this location, significant amounts of calcite and pyrite were observed. However, the occurrence of prehnite and laumontite, which are indicators of low permeability, before and in between the aquifer locations, may indicate reduced permeability zones.

4. HYDROTHERMAL ALTERATION

Hydrothermal alteration results from an interaction of the primary rocks and hot water and steam causing the dissolution of primary minerals, replacement and precipitation of new minerals and changes in permeability (Henley and Ellis, 1983). In all geothermal fields, the proper understanding of hydrothermal alteration is important as it is this information that gives the general picture of the geothermal system, its history and possibly its future (e.g. Njue, 2010). Also, hydrothermal minerals can be useful as geothermometers and, therefore, assist in determining the depth of the production casing while drilling. Additionally, these minerals are used in estimating fluid pH and other chemical parameters, as well as predicting the scaling and corrosion tendencies of fluids, measuring permeability and possible cold-water influx and as a guide to the hydrology (Reyes, 1990). The factors usually controlling alteration in geothermal systems are temperature, rock type, permeability, fluid composition and the duration of fluid-rock interactions (Browne, 1978; Elders et al., 1979).

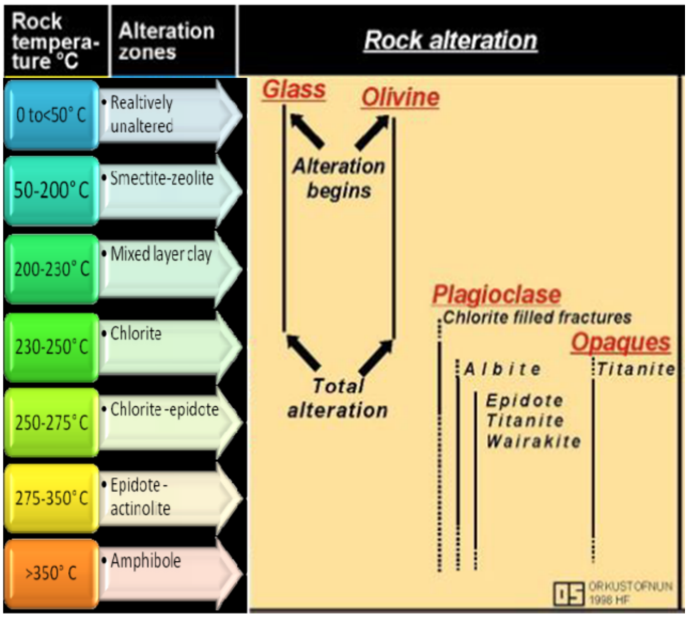

FIGURE 16: Mineral alteration-temperature diagram (modified from Franzson, 1998; and Franzson et al., 2010)

Temperature and permeability play the most important roles in the stability of most hydrothermal minerals. Temperatures vary from below 100 to 300°C. The source of permeability may be faults and fracture zones, lithological contacts, formation permeability (clasts and breccia fragments), and paleosols (Reyes, 2000). The compositions of fluids and gases are extremely variable. The mineralogical and alteration signatures may vary from one geothermal system to another. Detailed studies have contributed to the identification of various hydrothermal alteration zones and these are closely linked to the formation temperature (Figure 16). These zones are laid out using several temperature dependent minerals likely to deposit when at equilibrium with the surroundings. The principal components, glass and olivine, are the first to alter at low temperature, followed by plagioclase and pyroxene at much higher degrees and, finally, ore and high-temperature minerals above 200˚C (Franzson, 1998).

4.1 Alteration of primary minerals in well HE-32

A primary mineral in an igneous rock is any mineral that formed during the original solidification (crystallization) of the rock containing it, and retains its original composition and form. In contrast to primary minerals are secondary minerals, which form at a later time after the rock enclosing it has gone through processes such as metamorphism, weathering and hydrothermal alteration (Lapidus and Winstanley, 1987).

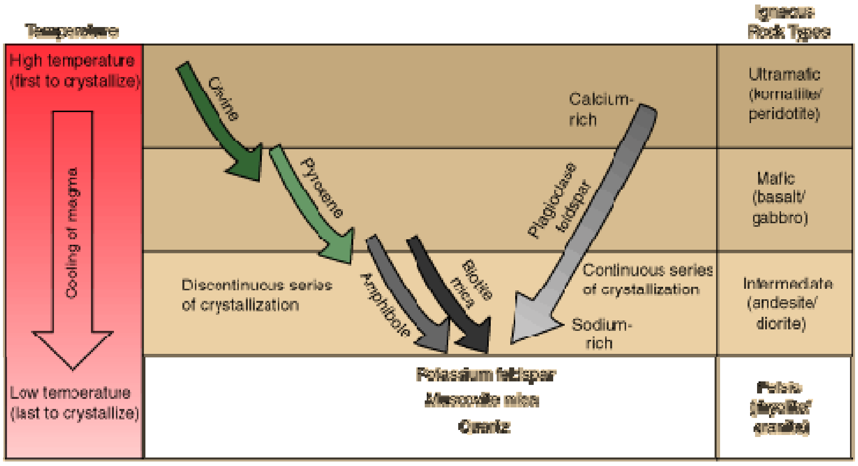

FIGURE 17: Bowen reaction series (2011)

Thus, primary minerals, crystallized from magma and governed by the physicochemical conditions under which the magma solidifies, become unstable in a geothermal environment where there is high permeability, elevated temperature and intense fluid activity. These minerals undergo chemical reactions with the hydrothermal fluids and readily alter to secondary minerals to become stable under the newly created natural conditions. The main primary minerals in Icelandic basaltic rocks are glass, olivine, plagioclase, pyroxene and opaques in order of their susceptibility to alteration (e.g. Gebrehiwot, 2010). The order of their alteration depends on the Bowen reaction series (Figure 17) so that the first mineral to be formed is also the first to be altered. Volcanic glass, which is a constituent of the basaltic rocks, cannot be classified as a mineral but is relevant in this discussion as its replacement products are quite relevant as hydrothermal minerals. The alteration of volcanic glass and the primary mineral assemblage of well HE-32 were studied under both binocular and polarizing microscope, mainly in the latter, and are described below.

Volcanic glass: By definition a mineral is a naturally-occurring solid with an ordered atomic arrangement and a chemical composition, which is fixed or which varies only within well-defined limits. An "ordered atomic arrangement“, i.e. atoms that are arranged in some geometric pattern, eliminates inhomogeneous solids such as glass (Mortensen and Hardarson, 2010) but, as noted above, is relevant in this discussion as replacement products are quite relevant as hydrothermal minerals. In the studied well, volcanic glass shows a highly vitreous lustre and has a good conchoidal fracture. It is the first constituent to be altered and replaced. It appears pale-brown in plain polarized light while it turns black in crossed polars. In all the thin sections analysed, on average 30% of the rock by volume is formed of glass, over 40% of which has been altered into palagonite, yellowish brownish in colour in both plain and crossed polars, but this varies highly with depth. However, in general, the replacement products of volcanic glass are zeolites (mordenite, laumontite), cristobalite, quartz, calcite and clays (Browne, 1984).

Olivine: It is one of the primary minerals that form basaltic rocks and it is very susceptible to alteration (Gebrehiwot, 2010). Raymond (1995) classified basaltic rocks based on olivine content as alkali olivine basalt or olivine basalt containing common to abundant olivine (and a Ca-pyroxene, augite), and tholeiitic basalt as one containing little or no olivine (and a Ca-poor pyroxene, orthopyroxene or pigeonite). In well HE-32, olivine was observed in small amounts, a maximum of 5% down to 392 m, after which it was completely replaced by calcite and clay. It was distinguished in thin section by its high birefringence, distinctive irregular fracture pattern and lack of cleavage. Moreover, the cracks in the crystals are quite characteristic as is the slight alteration of the mineral to mainly clays along the cracks or fractures. Additionally, the high relief of olivine against plagioclase was noticeable.

Plagioclase: It is the most abundant mineral occurring in most igneous rocks and a major mineral in basalt. Correspondingly, it was the most common mineral observed in well HE-32 where, on average, it occupied 10-20 % by volume of the rock. In crystalline rocks it mostly occurs as phenocrysts giving the rocks porphyritic textures. In ground mass, it occurs as tabular or needle like crystals which show an alignment probably of a flow texture, in which case it was interpreted as a tholeiitic basalt, for example at 202 and 392 m. It is readily identified by its low relief and conspicuous polysynthetic twinning. In well HE-32 plagioclase was observed to be progressively altered as temperature increased with depth and was finally replaced by albite and occasionally by calcite, zeolites, wairakite, and chlorite. The untwined plagioclase (albite), which resembles quartz, shows a characteristic brownish alteration or clouding which is not common in quartz. A substantial amount of plagioclase phenocrysts have liquid inclusions. Only albite could be identified with certainty; twinning is not common and when it occurs it is rather unique. The distinction between other varieties of plagioclase (oligoclase, andesine, labrodolite, bytownite, and anorthite) is rather detailed and is out of the scope of this study. It involves different optical methods, for example the Michel-Levy method, in which different maximum angles of extinctions of individual crystals are determined and averaged before referring them to curves of maximum extinction angles of plagioclase feldspars (Kerr, 1959).

Pyroxene: Pyroxenes are a group of minerals within the chain of silicates. A considerable range in chemical and corresponding optical properties prevails throughout the group which is, in general, composed of ortho pyroxenes (e.g. hyperthene, enstatite) and clinopyroxene (e.g. diopside, augite, pigeonite, wollastonite, etc.). However, the dominant pyroxenes that occur in Icelandic basalts are the clinopyroxenes, occurring mostly as phenocrysts and in the groundmass (Gebrehiwot, 2010). The pyroxenes resemble olivine but differ by the presence of better cleavage and inclined extinction. In well HE-32, the most common variety of pyroxenes is augite, observed both as phenocrysts and as part of the ground mass, the former being subhedral to euhedral in shape. It was observed to alter to both clay and smectite but never to actinolite which is a normal alteration product at higher temperatures. This is probably due to insufficient temperatures at the maximum depth at which cuttings could be obtained.

Opaque minerals: The iron oxides that occur as constituents of igneous rocks are magnetite, titanomagnetite, ilmenite, pyrite and rarely pyrrhotite (Hatch et al., 1972). However, it is of interest to note that in Icelandic basalts opaque minerals are mostly magnetite and some ilmenite (Hardarson pers. comm., 2011). In well HE-32 these minerals occur in minor amounts, normally less than 10% by volume in basaltic rocks and appear as opaques in both plane polarized and crossed polars in an optical microscope. These minerals can be adequately studied only with the aid of a metallurgical, as distinct from a petrological or microscopic approach (Hatch et al., 1972). However, in this study we were able to identify pyrite (sulphide) by its brassy yellow colour, euhedral crystals with square sections (cubic crystals) and high relief due to hardness (Kerr, 1959). Likewise, magnetite was recognised by its steel blue-black colour and octahedral, occasionally dodecahedral, crystals as distinct from its associate, ilmenite, which is violet black in colour with flake line crystals. They are generally more resistant to alteration except when altered sphene (titanite) is the main alteration product of these minerals. Sphene was not recognised in this study, however, it was observed in well HE-03, which is approximately 105 m away from HE-32 at 410 m depth, and becomes abundant below 700 m (Getaneh, 2001).

4.2 Distribution and description of hydrothermal alteration in well HE-32

The interaction between thermal fluids and rocks in geothermal systems produces a suite of secondary minerals whose identity and abundance depend on the prevailing physical and chemical conditions (e.g. Browne, 1993). This relationship is used to deduce reservoir conditions in addition to identifying minerals present in cuttings or cores. In some instances, a comparison between the deduced conditions and those actually measured will reveal that changes have occurred in a reservoir (Browne, 1993).

More important, perhaps, is that mineralogically deduced temperatures provide information on the thermal stability of a field. There are also some minerals that can be related to subsurface permeability (e.g. Section 3.6) and an early indication of well permeability can often be obtained by petrographic examination of cores and cuttings. This could be used, for example, in deciding casing depth, or in learning whether or not, or perhaps where, well damage has occurred (Njue, 2010).

Browne and Ellis (1970) described in considerable detail the factors that influence the distribution and kind of mineral assemblages present in hydrothermal systems. They include temperature, rock-water composition, pressure, duration of hydrothermal alteration and permeability. Whereas these factors are largely independent, the effects of one or more of the factors can exert a dominant influence in the location and extent of hydrothermal alteration. Temperature is the most significant factor in hydrothermal alteration because most of the chemical reactions require elevated temperatures. Accordingly, hydrothermal alteration of basaltic rocks in Icelandic geothermal areas proceeds very similarly in areas with meteoric thermal water and in areas with thermal brine (Kristmannsdóttir, 1975). The chemical composition of the host rock determines the availability of components to form alteration minerals as well as possible fugitive components from the presumed magmatic heat source. Although pressure affects hydrothermal alterations, depths penetrated by well HE-32, like in other geothermal fields elsewhere in the world, are not sufficient to greatly affect hydrothermal alteration mineral transformation (Browne and Ellis, 1970). Duration of the hydrothermal alteration at Hellisheidi geothermal field is not precisely known, but hydrothermal alteration is undoubtedly occurring at the present time and probably dates back at least to 0.3 M.y which, according to Franzson (1998), is the age of Mt. Hengill. Permeability of the rocks controls the access of thermal fluids, causing hydrothermal alteration of the rocks and precipitation of secondary minerals in open spaces. This fact is observed in basaltic rocks in Icelandic geothermal areas in which certain zones are heavily altered whereas nearby horizons are slightly altered, a factor attributed partly to differences in their permeability (Kristmannsdóttir, 1975). Additionally, rocks which have very restricted permeability or are completely impervious to fluid will be only slightly altered, as observed in dense lavas in the Olkaria Domes field in Kenya (Lagat, 2004). Crystallinity of the host rock is of importance because glass is more easily altered than crystalline rock. The chemical composition of the host rock determines the availability of components to form alteration minerals as well as possible fugitive components from the presumed magmatic heat source. Of the minerals in the basalts, olivine is most easily altered whereas plagioclase is the most resistant (Kristmannsdóttir, 1975).

In the Hellisheidi geothermal field, hydrothermal alteration minerals appear both as replacements of the primary minerals, as well as fillings in vesicles, vugs and fractures. Although hydrothermal alteration has changed the primary minerals in different ways and magnitudes, the original textures and mineral structures are often still recognizable. In this study, the distribution and abundance of hydrothermal minerals were obtained from the petrographic studies of drill cutting samples taken every 2 m, using both binocular and optical microscopes and XRD analysis of selected samples from well HE-32. Tabular results of XRD analyses and optical microscopy are attached in Appendix II and III, respectively.

Results indicate that the hydrothermal minerals occurring in well HE-32 include, but may not be limited to: limonite, siderite, zeolite groups occurring at different temperature ranges, calcite, pyrite, different types of clays, chalcedony, opal, quartz, albite, wairakite, prehnite, epidote, K-feldspar (adularia), wollastonite and garnet, although the latter three are in minor quantities (Figure 18). It is, however, of paramount importance to note that the most common amongst these are calcite, pyrite and clays. The abundance of calcite and pyrite may be due to the H_2S and CO_2 content commonly associated with geothermal systems. The different alteration minerals encountered in well HE-32 of the Hellisheidi high temperature geothermal field are described below:

Limonite is a mixture of natural oxides, but is not a true mineral; the oxides in it are predominantly goetheite and its variants. It forms by the oxidation of ferrous minerals, such as magnetite, which is found in all basalt. It is mostly in surface or near-surface conditions where there is abundant oxygen.

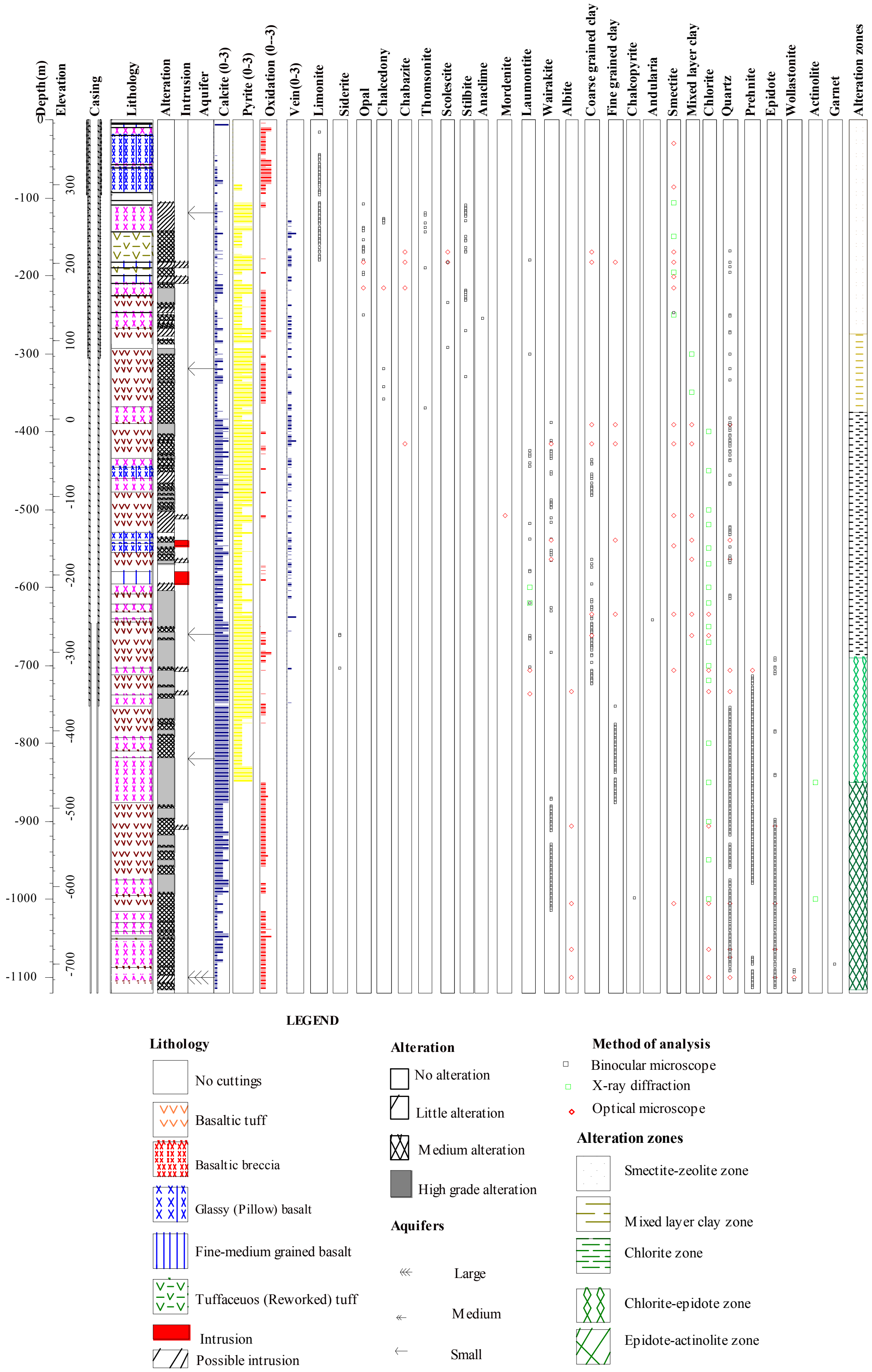

FIGURE 18: Lithological log and hydrothermal minerals and alteration zones of well HE-32

It is mostly associated with cold ground water systems. It was recognised in the studied well by its reddish-yellowish brown colour without a metallic lustre, opaque in cross polarised light and occasionally showing a concentric pattern in thin section. It was first observed at 16 m.

Siderite is an iron carbonate that forms small spherical shapes. It is mainly found in fissures in basalts where hot water has flowed, or with various ore minerals at the margins of intrusions (Saemundsson and Gunnlaugsson, 1999). In the studied well, siderite was observed between 660-662 m.

Opal is a silica mineral that is almost amorphous. It is softer and less dense than other silica minerals. It forms at low temperatures and hence is one of the amygdules found in the upper parts of the lava piles where it occurs in olivine basalts (Saemundsson and Gunnlaugsson., 1999). In the binocular microscope it was observed at two locations, 108 and 196 m, while in thin section it was seen at only two depths, 182 and 216 m where it was found to be transparent to sub-translucent, as a replacement to smectite, indicating a temperature below 100ºC.

Chalcedony is a silica mineral often regarded as amorphous but, in fact, it forms tiny thread-like crystals which are just distinguishable under a microscope. Its appearance indicates a temperature of about 120°C (Kristmannsdóttir, 1979). It occurs in thin section as a thin lining inside vesicles. It is colourless, grey to greyish blue and semi-transparent to translucent with a waxy lustre. It is progressively altered to quartz as temperature increases. In well HE-32 it could only be identified under binocular microscope where it was first seen at 126 m, at 150 m and disappeared after 358 m.

Zeolite group minerals comprise a category of hydrous secondary minerals composed of sodium, potassium and/or calcium-aluminium silicates. In dry air and when warmed slightly, they lose water, and reabsorb it under wet conditions (Saemundsson and Gunnlaugsson, 1999). They are formed by the chemical reaction of different types of volcanic rocks with alkaline groundwater (e.g. Gebrehiwot, 2010). The formation temperature of these minerals, with the exception of wairakite, ranges from about 40 to about 200°C (Table 3). In the studied well zeolites were not the most common secondary minerals but were by no means rare. As such, different varieties were identified at different depths and are summarized in Table 4.

Pyrite: Like calcite it is abundant in well HE-32 samples. It occurs as vein fillings and its occurrence can be used to infer permeability in a well (Browne, 1993).

TABLE 3: Some temperature dependent minerals in high-temperature areas in Iceland (Kristmansdóttir, 1979; Franzson, 1998)

Minerals	**Min. temp. (°C)**	**Max. temp. (°C)**
Zeolites	40	120
*Laumontite	120	180
*Wairakite	200	
Smectite		<200
**MLC	200	230
Chlorite	230	>300
Calcite	50-100	280-300
Quartz	180	>300
Prehnite	240	>300
Epidote	230-250	>300
Wollastonite	270	>300
Actinolite	280	>300

*Belong to the zeolite group
**Mixed-layer clay

Calcite: Calcite is precipitated from water solutions at all temperatures. Calcite formation can be linked to boiling, dilution and condensation of carbon dioxide in a geothermal system. It can also form during the heating of cooler peripheral fluids (Simmons and Christenson, 1994). In this study, this mineral is abundant and occurs in almost all lithologies and was quite easy to distinguish from quartz and plagioclase under binocular analysis, due to its effervescence in dilute hydrochloric. It is easily recognized under the petrographic microscope by its obvious cleavage and extreme birefringence. As a thermometer, calcite is useful because it becomes unstable at about 290°C and tends to disappear (Franzson, 2000).

TABLE 4: Occurrences of zeolites in well HE-32

Zeolite	**Characteristics**	**Occurrence in well HE-32**
Chabazite	Chabazite often is found filling vesicles. It is formed by white or clear near-cubic crystals. Crystals are often twinned, penetrating each other with rhomboid faces. Lustre is vitreous with uneven fractures.	Recognised in thin section at 170 and 182 m.
Thomsonite	Thomsonite occurs as circular radiating elongated, slightly flattened prismatic crystals, rather fibrous. It often fills vesicles or veins, very common in olivine basalts and is usually associated with the other zeolite minerals such as chabazite and phillipsite.	Seen in binoculars only at 370 m.
Mesolite/scolecite	Scolecite is structurally similar to mesolite and is characterised by a radial texture. These minerals are taken as a group as they form at a similar temperature range of 40-90°C. These minerals usually precipitate in vesicles as threads or hairs and are colourless and transparent. They occur at similar temperature and depth intervals as other zeolite group minerals such as stilbite, Thomsonite and chabazite.	They were observed in the binocular microscope and in thin sections at 170-182 m.
Stilbite	It was characterised in thin section by its perfect cleavage parallel to the plane of symmetry. The crystals are white and transparent to translucent, either colourless or white. It is an indicator of a minimum formation temperature of about 80°C.	Observed between but not throughout 130-330 m.
Analcime	Analcime forms colourless or white many sided (trapezohedral) crystals with vitreous lustre.	Observed in binocular microscope at 254 m.
Mordenite	Mordenite is generally white, but sometimes reddish-brown. It forms delicate flexible fibres and tufts which yield to the touch.	It was observed only at 508 m.
Laumontite	Laumontite is colourless or white and transparent. It has perfect cleavage and it is very brittle. It exhibits perfect cleavage with wedge shaped edges. It has a prismatic and fibrous structure and is mainly found as cavity fillings. It occurs in an unstable (usually below 200°C) form in vesicles, subsequently replaced by wairakite, epidote and quartz.	First appears at 110 m and is last seen at 708 m with intermittent occurrences in between the two depth intervals. Detected in XRD analysis at 196 m
Wairakite	It is has a very low relief, a dull dark gray colour and crosshatched twinning. It precipitates in veins or in the core of vesicles, usually succeeding the higher temperature minerals of epidote and quartz. It commonly replaces plagioclase and is observed to replace lower temperature zeolites. It is the only high-temperature zeolite, forming above 200°C (Saemundsson, and Gunnlaugsson, 1999).	It was first seen at 384 m depth and became abundant up to 1014 m. However, it is usually difficult to distinguish from analcime, especially in binocular analysis.

Fine-grained clay and coarse-grained clay: Fine-grained clay was first recognised under binocular as a fine layer of clay at 752 m; it is probable that it might have appeared at a shallower depth as generalised clay. In thin sections, however, it is seen as fine layers of clay mostly composed of smectite and mixed-layer clays radiating towards the centre of vesicles which they usually fill. On the other hand, coarse-grained clays have their edges and appear fibrous although more defined. They are presumably formed at higher temperatures than the fine-grained clay. In the investigated well, they are more abundant in cuttings between 450-750 m. In cases where the fine and coarse clays occur together, the latter overlays the former as they are formed later; this was observed in a thin section at 392 m.

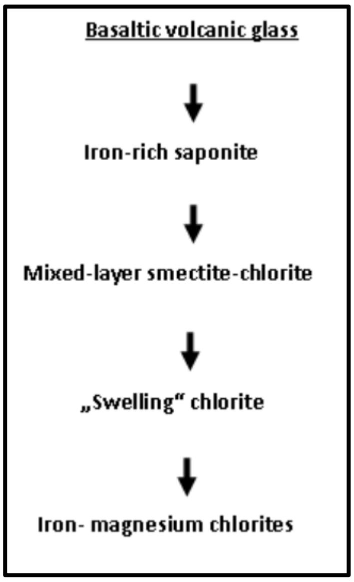

FIGURE 19: Alteration of volcanic glass (from Marosvolgyi, 2009)

Clays: The clay minerals are part of a general but important group within the phyllosilicates or sheet silicates that contain large percentages of water trapped between the silicate sheets. The chlorite minerals are sheet silicates, structurally related to clay minerals, but not included in the group of clay minerals (e.g. Marosvolgyi, 2009). The composition, structure and morphology of clay minerals depend on a number of environmental parameters – temperature, fluid composition/amount, pH, etc. (Njue, 2010). They are common and abundant alteration products in the hydrothermal systems, in both high- and low-temperature fields in Iceland (Kristmannsdóttir and Tómasson, 1978). Primary minerals like olivine, plagioclase and pyroxene are altered to different types of clays, depending on the temperature and permeability. Likewise, basaltic glass alters to chlorite of different chemical compositions as schematically illustrated in Figure 19. There are four distinguished main alteration zones in Icelandic geothermal fields. The first three zones are mainly characterized by a gradual transformation of trioctahedric Fe/Mg smectite (Fe-Mg rich saponite) to chlorite through the inter-layer smectite to smectite chlorite mixed-layer stage. These changes have been correlated with an alteration temperature of 200-250°C. Above this temperature (250-275°C), chlorite on addition to epidote is the dominant sheet-silicate; the change to the fifth alteration zone, which is the epidote-actinolite zone, occurs at temperatures of 275-350°C (Franzson, 2000). A correlation temperature of the alteration zones found in Icelandic high-temperature geothermal fields with tholeiite basaltic subsurface rocks and dilute water exists (Figure 16).

In our investigation, clays were analysed using the binocular microscope, petrographic microscope and XRD analysis and the three clay zones identified are listed below. (*Note:* Detailed results of XRD and optical microscopy are given in Appendices II and III, respectively.)

Smectite zone: Smectite is a low-temperature clay formed by the alteration of glass and ferromagnesian primary minerals such as olivine. Olivine and glass altered to clay, possibly smectite, as a replacement. Smectite also precipitates in pores and occurs as linings in vesicles at shallower depths. It was observed in binocular microscope to be generally brownish and greenish patches or as thin coatings in altered rocks at both 200 and 248 m, and as brownish colouration of a crystalline mass of relatively low birefringence lining vesicles in thin sections, analysed at a shallow depth of 30 m but still evident at 1006 m. In XRD, smectite clay was identified between 106-250 m where the rocks exhibited slight alteration. The smectite group of clays can be classified as swelling clays because they demonstrate high peak values in untreated and glycolated samples but designate lower values when heated. This indicates that the structure collapses with less moisture. The peak values are 13.30-14.91, 13.76-15.54 and 9.95-13.99 Å for untreated, glycolated and heated samples, respectively.

Mixed-layer clays are intermediate products of reactions involving the clay minerals end member in which the different kinds of clay layers alternate with each other. The reactions that produce mixed-layer clays are progressive high-temperature reactions altering smectite into chlorite via mixed-layer smectite/chlorite. The presence of mixed-layer clays indicates a temperature range of 200-230°C (Figure 16 and Table 3). It is quite difficult to distinguish mixed-layer clays from other clays which appear in almost all the cuttings analysed from well HE-32 under the binocular microscope. However, they were identified in a thin section at 182 m where they occur in a vesicle as a replacement mineral for plagioclase. In cross polarized light, they are strongly pleochroic exhibiting second order brown, orange and green colours. The more reliable results from XRD analysis detected mixed-layer clays between 275 and 375 m, showing peaks at 14.68-14.74 Å for the untreated and glycolated samples and collapsing to 12.33 Å in the heated samples, with an unchanged chlorite peak at 7.2 Å for all the runs.

Chlorites are generally green forming radiating, flaky or fibrous microscopic crystals or anhedral aggregates. The surface of the clay also appears very smooth compared to other clays under the petrographic microscope and can be fine or coarse grained. Chlorite is a common secondary mineral forming after mafic primary minerals or smectites and usually fills vesicles and occurs associated with quartz, epidote, prehnite and wollastonite. It marks a minimum temperature range of 230-250°C (Figure 16 and Table 3). It was detected between 564 and 1100 m in the thin section analysis where it was clearly distinguished by some of its features such as its green colour, being non-pleochroic under plane polarized light and its low birefringence with maximum interference colours rarely exceeding first order grey under crossed polars. In XRD analysis it shows two sets of results: chlorite (unstable) and chlorite (stable). Chlorite (unstable) has two close peaks at 15.39 and 14.38Å when the sample was untreated, glycolated and heated; the peak at 7.2 Å appeared when the sample was untreated and glycolated but disappeared completely when heated, thus the term unstable chlorite. On the other hand, chlorite (stable) showed two peaks, between 15.01 and 14.68 Å, and between 7.15 and 7.28 Å, when the sample was untreated, glycolated and heated.

Quartz is generally white-milky or even grey, and translucent or opaque. It has a vitreous lustre and an uneven or concoidal fracture. It forms prismatic hexagonal prismatic crystals which end in slanted faces meeting at a point. It occurs either as an alteration product of chalcedony or precipitates filling vesicles or as vein fillings together with epidote, prehnite, wairakite, pyrite and calcite. The first appearance of quartz represents a temperature of 180°C (Table 3). In thin section it was easy to distinguish it from feldspar because it is generally unaltered and lacks visible twinning or cleavage. Some of the crystals contained fluid inclusions and where they were small and numerous they gave the crystals a dusty appearance. Quartz first occurs at 168 m and thereafter well-developed crystals appear intermittently to the lowest depth where cuttings could be obtained in well HE-32.

Prehnite occurs mainly as vesicle and vein fillings but also as a replacement of primary minerals. In binocular microscope, it was identified by its rounded to nearly spherical shape, often occurring in clusters. It is white to colourless, brittle with an uneven fracture and has a vitreous to pearly lustre. In thin section, however, it was recognised by the characteristic strong birefringence (high-order interference colours) and a bow-tie structure. In the studied well, prehnite occurs in association with epidote, quartz and wairakite and was first observed at 714 m, thereafter becoming abundant down to 1116 m, indicating a minimum formation temperature of 240°C (Table 3).

Wollastonite is a mineral occurring with quartz, epidote and garnet in high-temperature systems and is characterised by white and fine fibrous aggregates filling vesicles. The first appearance of wollastonite marks a temperature of 270°C; it can be stable up to temperatures above 300°C (Table 3). In HE-32 it was identified by its hairy structure in the cutting analysis at 1090, 1094 and 1104 m while in thin section it was only recognised at 1100 m by its diagnostic property of showing interference colours extending up to first-order orange, together with the tendency for crystals to be elongated coupled with simple twinning along the longest crystal.

Actinolite belongs to the amphibole group of minerals. It is green to grey-green in colour, variable depending on the amount of iron. It is white and lustrous, silky to vitreous. It occurs as radiating or fibrous and very compact or as thin, very slender fibres, often radiating crystals. In thin section it is colourless, pale green to dark green showing pronounced pleochroism with moderate relief, the iron rich varieties being more pleochroic. There is a difference of opinion as to at what temperatures actinolite crystallizes, however the general opinion is that it indicates high-temperature systems between 280-300°C (Table 3). Actinolite was only detected by XRD analysis in HE-32 at 850 and 1000 m.

Garnet is a solid solution mineral with variable compositions between the common end members such as almandine, pyrope, andradite and grossular. In Iceland, garnet is mainly andradite (iron rich) and grossular (calcium-rich) and hydrogrossular, the only form that contains water. It is commonly orange red to brown in colour and occurs as subhedral crystal aggregates in highly altered rocks associated with actinolite, wollastonite, epidote, prehnite and quartz. It forms only at 300ºC and above (Saemundsson and Gunnlaugsson, 1999). It is very rare in the studied well as it was only seen at 1084 m in binocular analysis.

4.3 Veins and vesicle fillings in well HE-32

A vein is a tabular or sheet-like body of one or more minerals deposited in openings, joints or faults, frequently with associated replacement of the host rock. On the other hand, a vesicle is a small cavity in a glassy or phanitic igneous rock, formed by the expansion of a gas bubble during solidification of the rock (Lapidus and Winstanley, 1987). Despite their differences in structure and mode of formation, the general opinion is that both are vital in geothermal science since they are the sources of permeability (e.g. Browne, 1978). As such, their presence or absence in the well should be established during petrological studies of the subsurface lithology using both binocular and optical microscopes. It is also worthwhile to note that hydrothermal alteration minerals, known to be very important geothermometers, deposit within these structures. Vesicular rocks are common in Iceland where basaltic rocks predominate and, in HE-32, both vesicles and veins were identified and determined quantitatively (Figure 18). These structures gradually become filled with increasing alteration with limonite, siderite and low-temperature zeolites and other associated low-temperature clays or smectite and chalcedony. Clays predominantly occur as linings in vesicles as does calcite throughout the well.

4.4 Alteration zones in well HE-32

Progressive alteration of basaltic rocks in high-temperature geothermal areas leads to the formation of mineral alteration zones as expressed by their characteristic minerals. These zones are characterised by an abundance of particular minerals related to increased temperature and depth. Commonly, minerals used as geothermometers are zeolites, prehnite, garnet, clays and amphiboles (Browne, 1978, 1984). Based on studies of the alteration in well HE-32, five main alteration zones were distinguished, each zone being characterised by the dominance of particular minerals. The following description of these alteration zones is based on petrography and XRD clay analytical results. The reader is also referred to details of results in Appendix II.

Smectite-zeolites zone (0-275 m): This zone is characterised by the presence of smectite and zeolites indicating temperatures ranging between 50 and 200°C. The zeolites present are stilbite, scolecite/mesolite, laumontite and analcime. Calcite, pyrite, opal and chalcedony were also identified. One would probably be correct in demarcating the top of this zone at 30 m where smectite is quite evident in thin section, however this zone was extended to the top of a field in the study area due to evident altered clay, most likely smectite, around hot grounds a few metres away from the well under investigation. The lower boundary of this zone is the last appearance of smectite at 275 m.

Mixed-layer clays (275-375 m): This zone indicates a temperature range between 200 and 230°C (Figure 16 and Table 3) and extends beneath the smectite/zeolite zone down to 375 m where it occurs with chlorite. These clays are the intermediate products of reactions involving clay mineral end-members in which the different kinds of clay layers alternate with each other.

Chlorite zone (375-690 m): Chlorite is a high-temperature clay mineral which signifies a temperature range of 230-250°C and its first appearance marks the top boundary of this zone. Chlorite appears as a vesicle filling in this section. The first appearance of coarse-grained chlorite at 375 m defines the top boundary of the high-temperature zone. XRD clay analysis showed that this chlorite mineral was of an unstable variety, signified by the unchanged peaks 7-7.2Å for untreated and glycolated samples; it collapsed completely after being heated. Pyrite, calcite, mordenite, wairakite, and quartz occur in association with chlorite. Pyrite and calcite were still common together with the assemblage of analcime and quartz. The first appearance of chlorite indicates temperatures of about 230°C (Browne, 1978; Franzson, 1987).

Chlorite-epidote zone (690-850 m): This zone is marked by the first appearance of epidote at 690 m depth in thin section analysis, indicating temperature in excess of 250°C. Epidote continues to be present to the bottom of the well. It occurs either as a replacement product or as an alteration product of primary minerals, mainly plagioclase and pyroxene. The XRD analyses show that chlorite has an unstable behaviour and only stabilises at around 690 m. The mineral assemblages of quartz, wairakite, calcite, prehnite and pyrite are still present.

Epidote-actinolite zone (850-1116 m): This zone is defined by the first appearance of actinolite at 850 m which indicates a temperature range in excess of 275°C. Actinolite belongs to the amphibole group of minerals; it occurs as an alteration product of pyroxene. Quartz, wairakite, prehnite, epidote, wollastonite, pyrite, albite, actinolite and calcite are the main alteration minerals in this zone.

4.5 Mineral deposition and paragenesis of well HE-32

Paragenesis is a petrologic concept meaning an equilibrium assemblage of mineral phases. The paragenetic sequence in mineral formation is an important concept in deciphering the detailed geologic history of a geothermal system. In hydrothermal systems they are identified from cross-cutting veins and amygdale infilling sequences through detailed microscopic studies of petrologic thin section as well as macroscopic field relations and, at times, fluid inclusions. It is, however, of importance to note that due to the exclusive use of rotary bits and the fact that no cores were retrieved in the studied well, most of the macroscopic vein fillings and amygdale textures providing information on time relationships were lost. Nevertheless, we have attempted to reconstruct the paragenetic sequences of hydrothermal alteration minerals using thin section analysis from various depths in well HE-32 (Table 5). The depositional minerals were found mostly in vesicles. The sequence generally shows that the hydrothermal system has evolved from low- to high-temperature conditions. Chlorite, epidote, quartz, wairakite and wollastonite come later in the sequence, preceded by coarse grained, fine-grained and mixed-layer clay (Figure 20). It is possible to observe calcite in many of the mineral sequences, and at 416 m of the well it is commonly platy, a factor attributed to boiling conditions (Franzson, pers. comm.). Quartz is abundant below 700 m depth in H-32. However, it is usually not the last mineral to have formed in the mineral sequence in the lower part of the well, rather minerals such as epidote, calcite and at the maximum depth sampled, wollastonite.

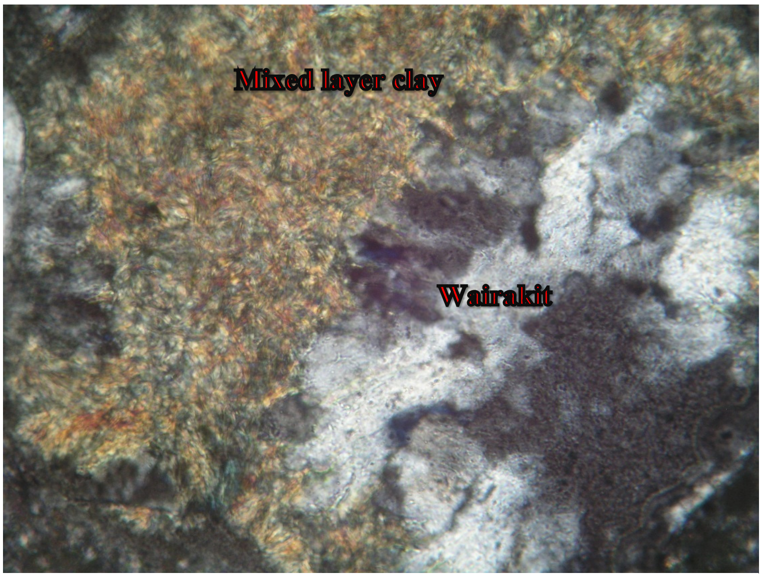

FIGURE 20: Wairakite suceeding mixed-layer clay in well HE-32 at 564 m

TABLE 5: Depositional sequences of hydrothermal alteration minerals in well HE-32
Explanation: sm=smectite, fgc=fine-grained clays, cgc=coarse-grained clays, mlc=mixed-layer clay me/so=mesolite/scolecite, chlc=chalcedony, chb=chabasite, qtz=quartz, wai=wairakite, wo=wollastonite, alb=albite, preh=prehnite, epi=epidote, cc=calcite and chl=chlorite

Depth (m)	Rock type	Earlier							Later
30	Tholeiitic basalt	sm							
86	Reworked tuff	fgc	sm						
170	Basaltic tuff	sm		me/sc					cc
182	Basaltic tuff	sm	chb						
		fgc	sm	chb					
		sm		me/sc					
202	Fine-grai. basalt	sm	cc	chlc					
216	Basaltic breccia	sm	chb	cgc					
		fgc	cgc						
392	Basaltic tuff	fgc	sm	chlc	cgc				cc
416	Basaltic tuff	sm		chb	cgc	wai			cc(pl)
508	Basaltic tuff	sm	mlc		chlc	wai			cc
540	Basaltic breccia	sm	mlc		cgc	wai			cc
564	Basaltic breccia	sm	mlc		cc	wai	chl		
634	Basaltic tuff	sm	mlc		cc		chl		cc
662	Basaltic tuff	sm					chl		cc
706	Basaltic breccia	sm			cgc		chl		cc
734	Basaltic tuff	sm			laum	qtz	chl		cc
906	Basaltic tuff	sm				alb	chl	preh	epi
1006	Basaltic tuff					alb	chl	qtz	epi
1064	Basaltic breccia						chl	qtz	epi
1074	Basaltic breccia						chl	qtz	cc
1100	Basaltic tuff							qtz	wo

4.6 Fluid inclusion geothermometry

When hydrothermal minerals grow, or recrystallize, in a fluid environment, tiny growth irregularities trap small amounts of the depositing fluid within the solid crystal. The sealing off of these irregularities yields primary inclusions or, by their later crystallization, perhaps in response to micro fractures, secondary inclusions (Browne, 1978). Secondary inclusions typically crosscut earlier generations (Shepherd et al., 1985). If the fluid trapped is a single phase, this will separate into a vapour (bubble) and a liquid at lower temperatures (two-phase boundary). It has been shown that heating of an inclusion on a heating stage will restore this fluid to single phase at its homogenization temperature. This is taken to be its entrapment temperature which is used to determine the thermal history of a reservoir (Browne 1978; Shepherd et al., 1985).

In our study, a total of 33 fluid inclusions in both quartz (3) and calcite (3) crystals were found in well HE-32 (Table 6 and Figure 21). The choice of depth at which fluid inclusions were taken was determined by the temperature curves (Figures 14 and 15). Thus, samples were taken before reaching the geothermal system, at the top of the system and within the system in order to get the overall temperature evolution of the geothermal reservoir. However, cuttings were too fine, especially beyond 1100 m and it was extremely difficult to find the required crystals. The two crystals thus obtained in the last depth interval were not polished as the usual procedure demands and parallel investigations are recommended for validation of the results.

TABLE 6: Fluid inclusion homogenization temperatures

Depth range (m)	No. of fluid inclusions	Homogenization temperature (T_h) ranges (°C)	Type of crystals
800-818	2	230-235	Calcite
	3	235-240	Calcite
	3	260-265	Quartz
	1	265-270	Quartz
	2	270-275	Calcite
	1	275-280	Quartz
	2	290-295	Quartz
	1	295-300	Quartz
1000-1010	1	235-240	Calcite
	8	275-280	Calcite
1098-1116	1	270-275	Quartz
	6	275-280	Quartz
	2	280-285	Quartz

The implication of the fluid inclusion temperatures in relation to the formation- and alteration temperatures are discussed in the next chapter.

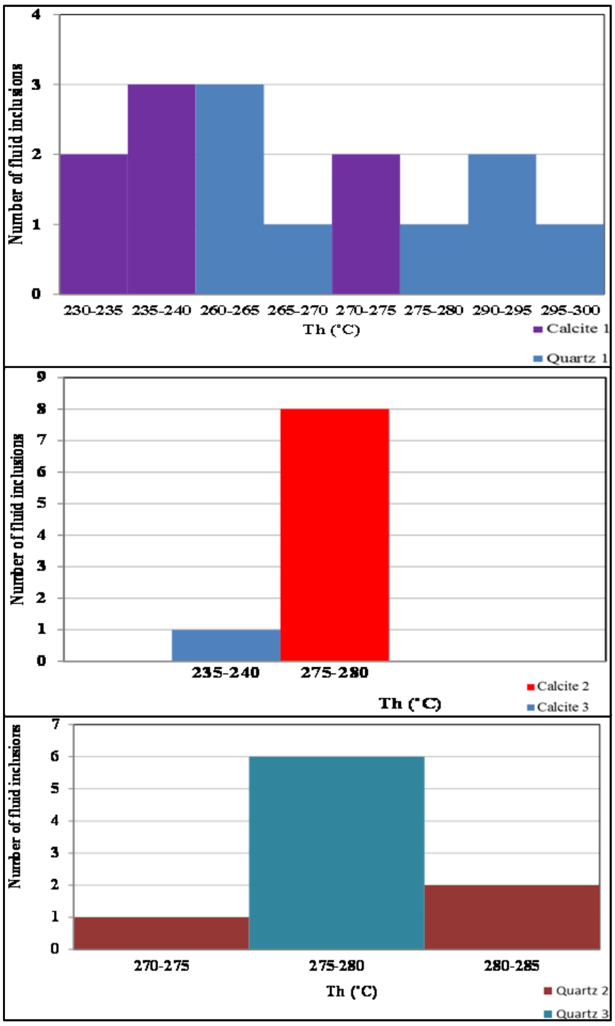

FIGURE 21: Histograms showing the variations of homogenization temperatures with depth; 800-818 m (top) 1000-1010 m (middle) and 1098-1116 m (bottom)

5. DISCUSSION OF RESULTS

Results from our investigation show that the subsurface geology of well HE-32 is predominantly made of hyaloclastites, composed of tuffs (basaltic and reworked), basaltic breccias and pillow (glassy) basalt. Relatively thin, fine- to medium-grained crystalline basalts represent interglacial lava flows and intrusive rocks. Except for the first 20 m basalt layer, which belongs to the postglacial lavas of 5500 and 2000 years age, and the first hyaloclastite formation, possibly the base of Mt. Stóra Skardsmýrarfjall, which is from the last glaciation and thus, younger than 115,000 years, it is not easy to estimate the age of the other formations below. However, it can be said that they are > 115,000 years (Getaneh., 2001), and an age of 0.3 m.y. has been postulated for Mt. Hengill and the associated geothermal activity in the area (Franzson, 1998).

The temperature evolution of the geothermal reservoir into which well HE-32 was drilled has been evaluated in four different, but complimentary ways: (1) the hydrothermal alteration temperature, which was assessed according to the first appearance of the different, temperature-dependent alteration minerals, (2) the formation temperature, estimated from the heating-up (after drilling) temperature logs, (3) the homogenization temperature of fluid inclusions and (4) the calculated boiling point temperature curve (calculated as the saturation temperature, using steam tab software, density, acceleration due to gravity, depth and atmospheric pressure as input parameters).

The alteration mineral distribution of the well shows a trend where low-temperature minerals, like zeolites, form in the upper part of the well and are gradually replaced by moderate-temperature minerals, like quartz and wairakite, which are followed at greater depth by high-temperature mineral assemblages like chlorite, prehnite, epidote, wollastonite, actinolite and garnet. This is a similar high-temperature assemblage as that found at Nesjavellir at the northern sector of Hengill Mountain (Franzson, 2000). Based on the temperature-dependent minerals and their first appearance, the alteration was divided into five zones: zeolite-smectite, mixed-layer clay, chlorite, chlorite-epidote and epidote-actinolite zones. The mineral deposition sequence generally shows that the hydrothermal system has evolved from low- to high-temperature conditions. Chlorite, epidote, quartz, wairakite and wollastonite appear later in the sequence, preceded by coarse-grained, fine-grained and mixed-layer clay.

The formation temperature curve of the well shows a progressive temperature increase with depth for the first 900 m, thereafter a reversal occurs down to the bottom (Figure 22).

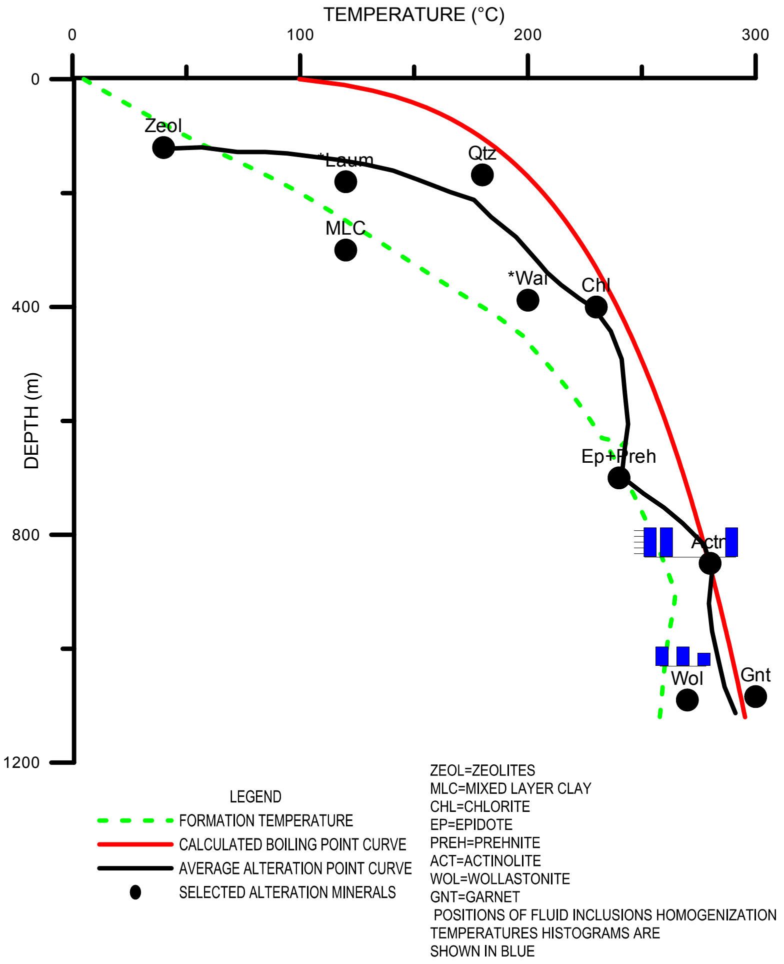

FIGURE 22: Formation, hydrothermal alteration, calculated boiling point and homogenization temperatures of well HE-32

As for homogenization temperatures, we have 3 histograms of fluid inclusions from 800-81, 1000-1010 and 1098-1116 m depths (Figures 21). In general, the investigated 33 fluid inclusion temperatures in both quartz and calcite crystals in well HE-32 ranged from 230 to 300°C which, in a general sense, may imply that the system is in equilibrium with the formation temperature (Table 6 and Figure 22). However, at depths between 800 and 818 m, fluid inclusions indicate that the equilibrium condition of the system were at one time 300°C, notably higher than the present formation temperature and the boiling point; the system has, therefore, cooled by about 10°C with time. This argument is supported by the fact that actinolite is present at around this depth, where the measured temperature today is ~262°C (Figure 22). This is 18°C lower than the normal temperature stability range of actinolite (≥280°C). The increased alteration at this depth could be associated with an aquifer in this zone (Figure 10) which has subsequently cooled. Above 1000 m, the variation of the present temperature (~260°C) with fluid inclusion homogenization and temperatures show cooling of about

15-18°C, whereas the occurrence of wollastonite and garnet with respective stabilisation temperatures of 270 and 300°C in the vicinity indicate cooling of the system by 10-40°C. Furthermore, the alteration temperature curve of the well shows a progressive temperature increase with depth, generally higher than the formation temperature curve (Figure 22), emphasizing that the reservoir has been cooling with time.

Moreover, the increased separation of the calculated boiling point curve and the formation temperature curve further demonstrates that the system is increasingly being far from boiling with depth. The high temperature as recorded by the fluid inclusions is likely to be near the boiling point, interpreted to indicate the boiling condition in the geothermal system during their entrapment. Again, the increased alteration and the relatively large aquifer located at around 1100 m (Figure 15) are the most plausible causes of cooling. Additionally, the abundance of prehnite, a low-permeability indicator mineral, between 700 and 1100 m may be due to poor permeability in the well, thus requiring more time before the alteration mineralogy can equilibrate to the new temperature conditions. In general, from Figure 22, we can say that the system has been cooling as alteration temperatures are higher than formation temperatures.

An attempt was made to correlate the lithological units of the three wells drilled on the same well pad (Figure 23). This revealed curious similarities, for example, intrusions associated with moderate to

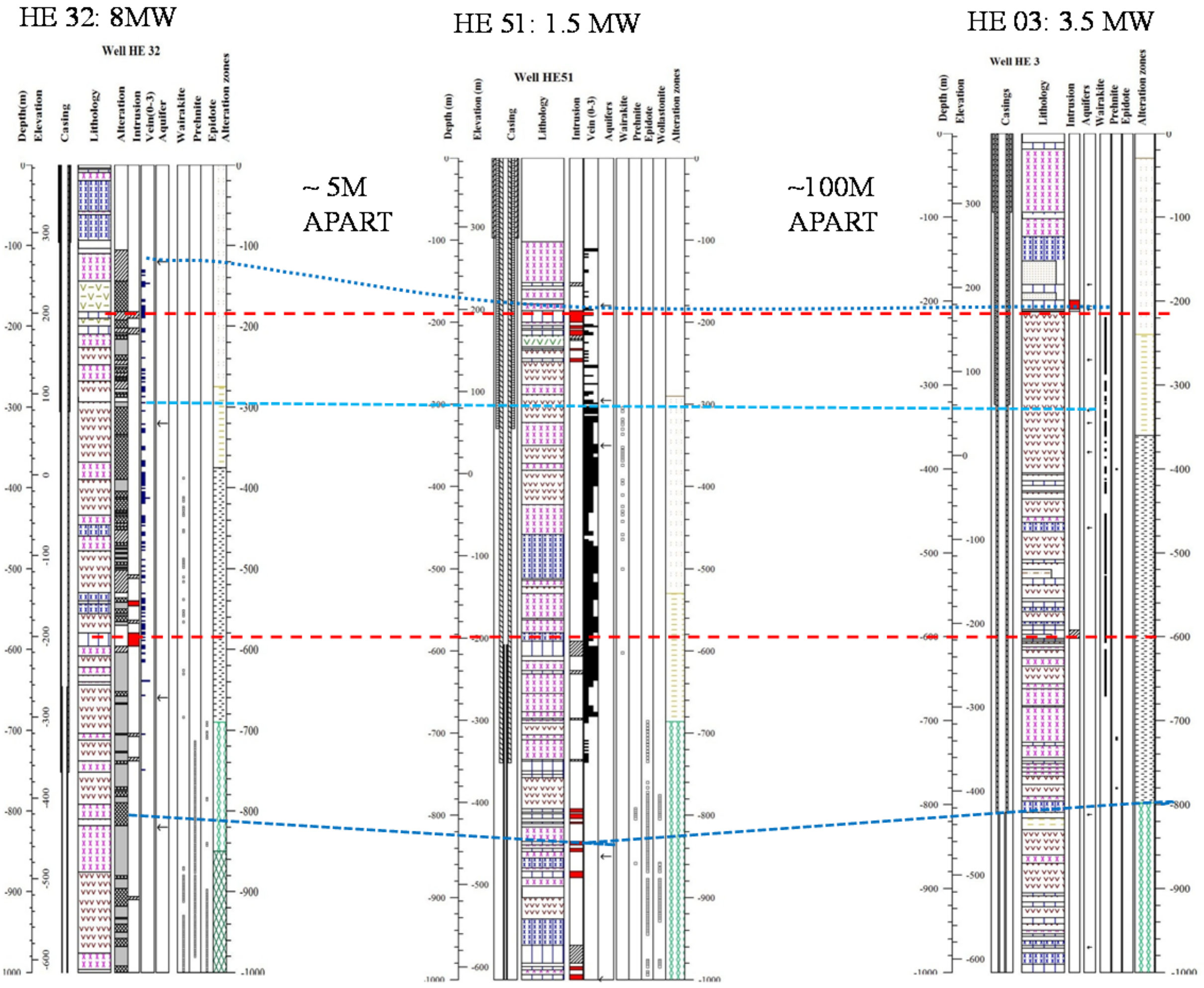

FIGURE: 23. Relationships between well HE-32, HE-3 and HE-51; note the same lithology, hydrology (blue lines) and intrusions (red lines); for legend of lithology, see Figure 18 (source for well HE-51, Matthíasdóttir and Ingólfsson, 2010 a, b; for well HE-3, data is partly modified from Getaneh, 2001 and Jónsson et al., 2001) high frequency of veins and fractures occur at similar depths (200 and 600 m) and around these depths aquifers are found in all 3 wells.

This study has involved the prediction of geological formations below 1116 m, where total loss of circulation occurred, by using geophysical logs. Natural gamma counts, neutron-neutron and resistivity logs showed no or minor variations beyond 1450 m; this limited our ability to subdivide the predicted fine- to medium-grained basalt beyond this depth. The fine- to medium-grained basalt may be the interglacial basalt, as assumed in developed cross-sections of the area, although well HE-32 is excluded (Figure 23).

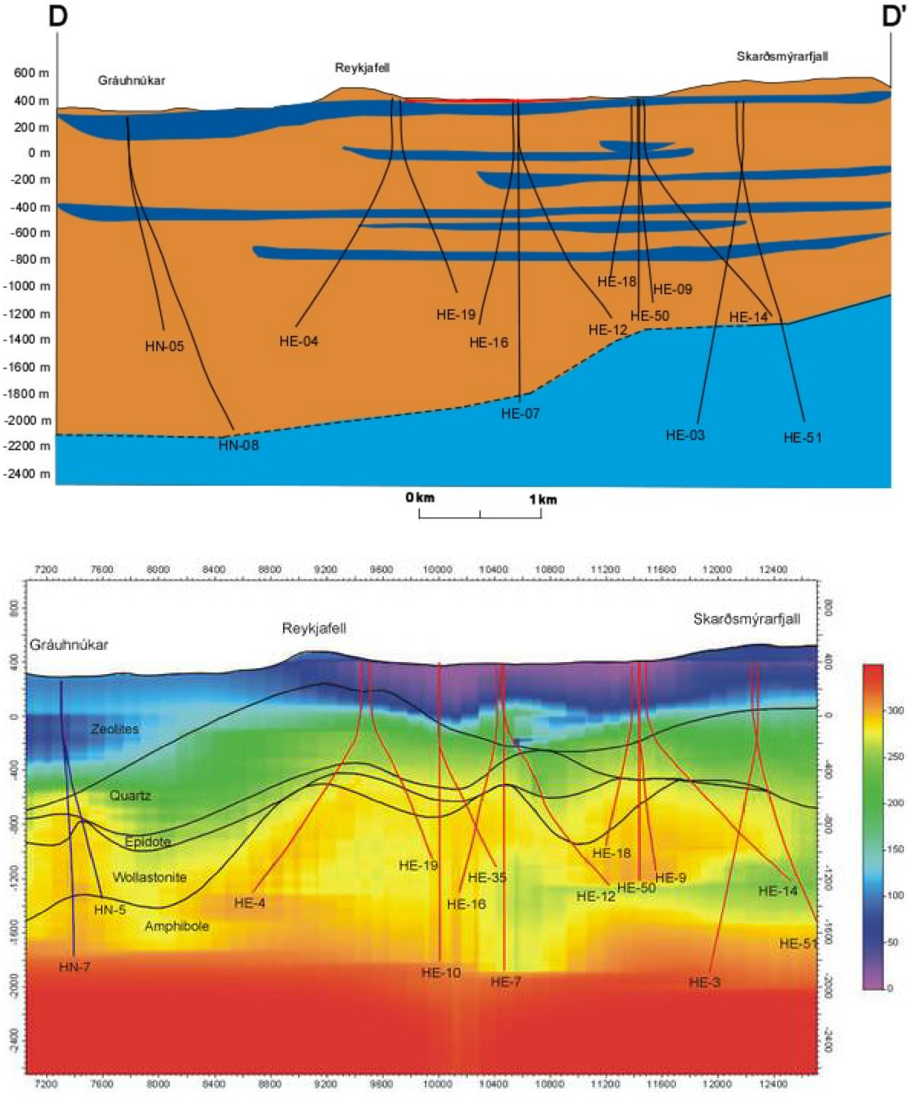

FIGURE 24: Geological (upper) and formation temperature (lower) cross-sections including wells HE-3 and HE-51. In the geological cross-section, blue formations are interglacial lava series and the light blue formation is interpreted as the bottom of the Hengill central volcano; red formations are postglacial lava; while brown formations are hyaloclastite formations. Dotted, black line represents areas where no data is available (Helgadóttir et al., 2010)

Hydrothermal mineral distributions in the three wells showed some similarities but some differences were also apparent (Figure 23). While wairakite occurs in all the wells, its first appearances are at about 380, 280 and 210 m in well HE-32, HE-51 and HE-3, respectively. In a similar way wollastonite is found at ~770 m depths in HE-51, whereas in it was first encountered at 1090 m in HE-32 and it is absent in HE-3. This implies that hydrothermal mineral distribution recorded in well HE-32 fits in the wave-like pattern (Figure 24) observed in the nearby wells. Moreover, the depth and extent of the alteration zones vary in both extent and depth, being shallower in well HE-32 but smaller in extent than in well HE-3 which is, in turn, shallower than in well HE 51. This implies that well HE-32 is hotter than HE-3 which is, in turn, hotter than HE-51. Accordingly, the production capacities of the three wells are 8, 3.5 and 1.5 MWe, respectively, at 8 bar pressure (Reykjavik Energy, unpublished data).

6. CONCLUSIONS

From this study the following can be deduced:

- The litho-stratigraphy of well HE-32 of the upper 1116 m consists predominantly of hyaloclastites, with a few thin intercalated basalt lavas and three minor basaltic intrusions.
- Using geophysical logs, prediction of the formations below 1116 m, where total circulation loss occurred, indicates the repetition of the same formation (hyaloclastites) down to about 1500 m beyond which fine- to medium-grained basalt seems to be the dominant rock formation.
- Furthermore, this study has re-emphasized the contribution of geophysical logs in both the modification of the lithology, by cuttings analysis, and the prediction of lithology where total loss of circulation may be encountered, especially in the production part of the well.
- The alteration mineral distribution of HE-32 shows a trend where low-temperature minerals, like zeolites, form in the upper part of the well and are gradually replaced by moderate-temperature minerals like quartz and wairakite, which are followed at greater depths by high-temperature mineral assemblages like chlorite, prehnite, epidote, wollastonite, actinolite and garnet.
- The alteration mineral assemblage and distribution study indicates the presence of five temperature related alteration zones. These are: a smectite-zeolite zone (50-200°C); a mixed-layer clay zone (200-230°C); a chlorite zone (230-250°C); a chlorite-epidote zone (250-275°C); and finally an epidote-actinolite zone (275-350°C).
- According to the hydrothermal alteration minerals, the temperature showed a progressive increase with depth, first with the appearance of minerals such as low-temperature zeolites, quartz (not low), and smectite. The alteration increased below 388 m depth with the appearance of quartz (≥180°C), wairakite (≥200°C) and later epidote (≥230°C) at 690 m. The alteration increased below 850 m depth (appearance of actinolite, ≥280°C) and localized at around 1084 m depth (+garnet, ≥300°C).
- Comparison of alteration mineral temperature and measured temperature showed that the alteration temperature is, in general, higher than but close to the formation temperature; one can generally conclude that the geothermal system is overall in equilibrium with a reservoir temperature of 230-270°C down to around 850 m, although temperatures as high as 300°C were recorded by a few fluid inclusions. There was a localized ~40°C cooling at the aquifer zones at 800-1100 m depth. Abundant prehnite at 700-1100 m depth may be due to low permeability.
- According to circulation loss data, drillers' logs and alteration, three small aquifers above the production casing were recognized and five aquifers were identified in the production section, two small, two medium and one large. In general, aquifers in the first 1100 m are associated with lithological contacts and intrusion contacts.
- We have learnt from the investigation of well HE-32 and, in addition, the comparison with wells HE-3 and HE-51, which were drilled on the same well pad, that whereas a relationship in the overall subsurface geology may exist in the neighbouring wells, each well is independent and behaves as an individual.

ACKNOWLEDGEMENTS

I am sincerely grateful to the UNU-GTP and the Government of Iceland for the fellowship to attend this course and all the personalities involved in one way or another in achieving this objective. To the UNU Geothermal Training Programme staff, Dr. Ingvar B. Fridleifsson, Mr. Lúdvík S. Georgsson, Ms. Thórhildur Ísberg, Mr. Ingmar G. Haraldsson and Mr. Markús A.G. Wilde – words cannot express my gratitude.

One cannot imagine how this manuscript would be without the timely responses and patience of my advisors, Dr. Björn S. Hardarson and Dr. Hjalti Franzson. Their contributions in the specialized lectures and throughout the project are highly acknowledged. Ms. Anette K. Mortensen, Gudmundur, Christa, Sigurdur and Signý plus the entire Iceland GeoSurvey (ÍSOR) staff: thank you very much indeed for taking time off your busy schedules to share your skill and knowledge.

Reykjavik Energy is gratefully acknowledged for allowing access to data for the wells of this study.

I acknowledge my employer, Ministry of Energy and Mineral Development: Department of Geological survey and Mines and, in particular, the Permanent Secretary, for granting me permission to attend this training. My very sincere gratitude goes to my loving family and friends back home in Uganda for their encouragement and prayers. My gratitude goes to my wife, for her prayers, patience and single parenthood of our children.

Thanks to all the 2011 UNU Fellows for the ideas and good moments we shared during the entire 6-month period. Special acknowledgements go to Jean and Victor with whom I shared the apartment for a calm environment and to the borehole geology classmates Ngereja and Convine for sharing their knowledge, skills and experiences during this course.

REFERENCES

Árnason, K., Eysteinsson, H., and Hersir, G.P., 2010: Joint 1D inversion of TEM and MT data and 3D inversion of MT data in the Hengill area, SW Iceland. *Geothermics, 39,* 13-34.

Árnason, K., Karlsdóttir, R., Eysteinsson, H., Flóvenz, Ó.G., and Gudlaugsson, S.Th., 2000: The resistivity structure of high-temperature geothermal systems in Iceland. *Proceedings of the World Geothermal Congress 2000, Kyushu-Tohoku, Japan,* 923-928.

Ásmundsson, R.K., 2011: *Borehole investigations in geothermal systems.* UNU-GTP, Iceland, unpublished lecture notes.

Björnsson, A., 1990: *Geothermal research. A review of the nature of geothermal fields, exploration and production* (in Icelandic). Orkustofnun, Reykjavík, report OS-90020/JHD-04, 50 pp.

Björnsson, A., Axelsson, G., and Flóvenz, Ó.G., 1990: The origin of hot springs in Iceland. *Nátturufraedingurinn, 60* (in Icelandic), 15-38.

Björnsson, A., Saemundsson, K., Sigmundsson, F., Halldórsson, P., Sigbjörnsson, P., and Snaebjörnsson, J.T., 2007: *Geothermal projects in NE-Iceland at Krafla, Bjarnarflag, Gjástykki and Theistareykir. Assessment of geo-hazards affecting energy production and transmission systems emphasizing structural design criteria and mitigation of risk.* Landsvirkjun, Reykjavík, report LV-2007/075, 42 pp.

Bödvarsson, G., and Pálmason, G., 1961: Exploration of subsurface temperatures in Iceland. *Jökull, 11,* 39-48.

Bowen Reaction Series, 2011: Process of crystalization of igneous rocks from magma. Website: *www.geophy/bowen.html.*

Browne, P.R.L., 1978: Hydrothermal alteration in active geothermal fields. *Annual Reviews of Earth and Planetary Science, 6,* 229-250.

Browne, P.R.L., 1984: *Lectures on geothermal geology and petrology.* UNU-GTP, Iceland, report 2, 92 pp.

Browne, P.R.L., 1993: Application of mineralogical methods to assess the thermal stabilities of geothermal reservoirs. *Proceedings of the 18th Workshop on Geothermal Reservoir Engineering, Stanford University, Stanford, CA,* 73-78.

Browne, P.R.L., and Ellis, A.J., 1970: The Ohaki-Broadlands hydrothermal area, New Zealand: Mineralogy and related geochemistry. *Am. Jour. Sci., 269, 97-131.*

Elders, W.A., Hoagland, J.R., and McDowell, S.D., 1979: Hydrothermal mineral zones in the geothermal reservoir of Cerro Prieto. *Geothermics, 8,* 201-209.

Franzson, H., 1987: The Eldvörp high temperature area, SW Iceland. Geothermal geology of first exploration well. *Proceedings of the 9th NZ Geothermal Workshop, Auckland, NZ, 179-185.*

Franzson, H., 1998: Reservoir geology of the Nesjavellir high-temperature field in SW-Iceland. *Proceedings of the 19th Annual PNOC-EDC Geothermal Conference, Manila*, 13-20.

Franzson, H., 2000: Hydrothermal evolution of the Nesjavellir high-temperature system, Iceland. *Proceedings of the World Geothermal Congress 2000, Kyushu-Tohoku, Japan,* 2075-2080.

Franzson, H., Árnason, K., Saemundsson, K., Steingrímsson, B., and Gunnlaugsson, E., 2010: The Hengill geothermal system, conceptual model and thermal evolution. *Proceedings of the World Geothermal Congress 2010, Bali, Indonesia,* 9 pp.

Gebrehiwot M., K., 2010: *Subsurface geology, hydrothermal alteration and geothermal model of Northern Skardsmýrarfjall, Hellisheidi geothermal field, SW Iceland.* University of Iceland, MSc thesis, UNU-GTP, Iceland, report 5, 65 pp.

Getaneh, E., 2001: Borehole geology and alteration mineralogy of the upper half of well HE-3, Hellisheidi geothermal field, SW-Iceland Report 4 in: *Geothermal training in Iceland 2001.* UNU-GTP, Iceland 59-82.

Hardarson, B.S., Einarsson, G.M., Kristjánsson, B.R., Gunnarsson, G., Helgadóttir, H.M., Franzson, H., Árnason, K., Ágústsson, K., and Gunnlaugsson, E., 2010a: Geothermal reinjection at the Hengill triple junction, SW Iceland. *Proceedings of the World Geothermal Congress 2010, Bali, Indonesia,* 7 pp.

Hardarson, B.S., Sigurgeirsson, M.A., Tryggvason, H., and Feucht, C., 2010b: *Hellisheidi, well HE-32: Pre-drilling 1st and 2nd phase: Drilling for surface casing to 98 m, anchor casing to 307 m and production casing to 752 m depth.* ÍSOR – Iceland GeoSurvey, report ÍSOR-2010/090 (in Icelandic), 43 pp.

Hardarson, B.S., Sigurgeirsson, M.A., Tryggvason, H., Nielsson, S., and Gudbrandsson, S., 2010c: Hellisheidi, well HE-32: *3rd phase drilling with 9 5/8′′ production liner from 752 m to 2465 m depth.* ÍSOR – Iceland GeoSurvey, report OS-2010/091 (in Icelandic), 37 pp.

Hatch, F.H., Wells, A.K., and Wells, M.K., 1972: *Petrology of igneuos rocks* (13th edition). George Allen and Unwin Ltd., London, 551 pp.

Helgadóttir, H.M., Snaebjörnsdóttir, S.A., Níelsson, S., Gunnarsdóttir, S.H., Mattíasdóttir, T., Hardarson, B.S., Einarsson, G.E., and Franzson, H., 2010: Geology and hydrothermal alteration in the reservoir of the Hellisheidi high temperature system, SW-Iceland. *Proceedings of the World Geothermal Congress 2010, Bali, Indonesia,* 10 pp.

Helm-Clark, C.M., Rodgers, D.W., Smith, R.P., 2004: Borehole geophysical techniques to define stratigraphy, alteration and aquifers in basalt. *J. Applied Geophys., 55,* 3-38.

Henley, R.W., and Ellis, A.J., 1983: Geothermal systems ancient and modern: a geochemical review. *Earth Science and Reviews, 19,* 1-50.

Jakobsson, S., Jónasson, K., and Sigurdsson I.A., 2008: The three igneous rock series of Iceland. *Jökull, 58, 117-138.*

Jónsson, S.S., Steingrímsson, B., Gudmundsson, B., Hermannsson, G., Fridleifsson, G.Ó., Franzson, H., Birgisson, K., Sigurdsson, Ó., and Gudlaugsson, S.P., 2001: Hellisheidi, well HE-3. *2nd Phase drilling for 9 5/9´´ production casing from 324 m to 812 m depth.* Orkustofnun, Reykjavík report OS-2001/053 (in Icelandic), 41 pp.

Kerr, P.F., 1959: *Optical mineralogy* (3rd edition). McGraw-Hill Book Co., NY, 442 pp.

Khodayar, M., and Franzson, H., 2007: Fracture pattern of Thjórsárdalur central volcano with respect to rift-jump and a migrating transform zone in S-Iceland. *J. Structural Geol., 29-5,* 898-912.

Koestono H., 2007: Borehole geology and hydrothermal alteration of well HE-24, Hellisheidi geothermal field, SW-Iceland. Report 10 in: *Geothermal Training in Iceland 2007.* UNU-GTP, Iceland, 199-224.

Kristmannsdóttir, H., 1975: Hydrothermal alteration of basaltic rocks in Icelandic geothermal areas. *Proceedings of the 2nd U.N. Symposium on the Development and Use of Geothermal Resources, San Francisco,* 441-445.

Kristmannsdóttir, H., 1979: Alteration of basaltic rocks by hydrothermal activity at 100-300°C. In: Mortland, M.M., and Farmer, V.C. (editors). *International Clay Conference 1978*. Elsevier Scientific Publishing Co., Amsterdam, 359-367.

Kristmannsdóttir, H., and Tómasson, J., 1978: Zeolite zones in geothermal areas in Iceland. In: Sand, L.B., and Mumpton (editors), *Natural zeolites, occurrence, properties, use*. Pergamon Press Ltd., Oxford, 277-284.

Lagat, J.K., 2004: *Geology, hydrothermal alteration and fluid inclusion studies of the Olkaria Domes geothermal field, Kenya.* University of Iceland, MSc thesis, UNU-GTP, Iceland, report 2, 71 pp.

Lapidus, D.F., and Winstanley, I., 1987: *Collins dictionary of geology*. Harper Collins Publishers, London and Glasgow 565 pp.

Low, J.W., 1977: Examination of well cuttings and the lithologic log. In: Leroy, L.W., Leroy, D.O., and Raese, J.W. (eds.), *Subsurface geology* (4th ed.). Colorado School of Mines, Golden, Colorado, 286-303.

Marosvölgyi, K., 2009: *Retrograde alteration of basaltic rocks in the Theistareykir high-temperature geothermal field, North-Iceland.* University of Iceland & the University of Akureyri and RES - School for Renewable Energy Science, Akureyri, MSc thesis, 41 pp.

Matthíasdóttir, T., and Ingólfsson, H., 2010a: *Hellisheidi, well HE-51: Pre-drilling 1st and 2nd phase: Drilling for surface casing to 98 m, anchor casing to 330 m and production casing to 737 m depth.* ÍSOR – Iceland GeoSurvey, Reykjavík, report ÍSOR-2010/108 (in Icelandic), 47 pp.

Matthíasdóttir, T., and Ingólfsson, H., 2010b: *Hellisheidi, well HE-51: 3rd phase drilling with 8½" drill bit for 7" liner from 737 m to 2620 m depth.* ÍSOR – Iceland GeoSurvey, Reykjavík, report OS-2010/109 (in Icelandic), 52 pp.

Mbia, P.K., 2010: Borehole geology and hydrothermal mineralisation of well HE-39, Hellisheidi geothermal field, SW-Iceland. Report 19 in: *Geothermal training in Iceland 2010.* UNU-GTP, Iceland, 337-364.

Mortensen, A.K., and Hardarson, B.S., 2010: *Notes on mineralogy*. Course for Geoscientific Exploration of Geothermal Resources, Olkaria, Kenya, UNU-GTP and KenGen.

Mostaghel, B., 1999: Processing and interpretation of geophysical well logs from well KJ-32, Krafla geothermal field, NE-Iceland. Report 8 in: *Geothermal training in Iceland 1999.* UNU-GTP, Iceland, 193-220.

Njue, M.L.M., 2010: Borehole geology and hydrothermal mineralisation of well HE-27, Hellisheidi geothermal field, SW-Iceland. Report 24 in: *Geothermal training in Iceland 2010.* UNU-GTP, Iceland, 463-492.

Quintero Roman, R.M., 2010: Borehole geology of well SJ9-2 San Jacinto – Tizate geothermal field, NW-Nicaragua. Report 27 in: *Geothermal training in Iceland 2010.* UNU-GTP, Iceland, 563-588.

Raymond, L.A., 1995: *Petrology, the study of igneous, sedimentary and metamorphis rocks* (2nd ed.). McGraw-Hill Co., Inc, NY, 720 pp.

Reyes, A.G., 1990: Petrology of Philippine geothermal systems and the application of alteration mineralogy to their assessment. *J. Volc. Geoth. Res., 43,* 279-309.

Reyes, A.G., 2000: *Petrology and mineral alteration in hydrothermal systems from diagenesis to volcanic catastrophes*. UNU-GTP, Iceland, report 18-1998, 77 pp.

RockWare Inc., 2007: *LogPlot program*. RockWare, Inc.

Saemundsson, K., 1979: Outline of the geology of Iceland. *Jökull 29,* 7-28.

Saemundsson, K. 1995: *Hengill geological map (bedrock) 1:5000*. Iceland GeoSurvey.

Saemundsson, K., and Gunnlaugsson, E., 1999: *Icelandic rocks and minerals*. Edda and Media Publishing, Reykjavík, Iceland, 233 pp.

Senior, A.L., Cinotto, J.P., Conger, W.R., Bird, H.P., and Pracht, A.K., 2005: *Interpretation of geophysical logs, aquifer tests, and water levels in wells in and near the North Penn Area 7 Superfund site, Upper Gwynedd Township, Montgomery County, Pennsylvania*. US Geological Survey, scientific investigations report, 2005-5069, 2000-02.

Shepherd, T.J., Rankin, A.H., and Alderton, D.H.M., 1985: *A practical guide to fluid inclusion studies.* Blackie and Son, Glasgow, UK, 239 pp.

Simmons, S.F., and Christenson, B.W., 1994: Origin of calcite in a boiling geothermal system. *Am. Jour. Sci., 294,* 361-400.

Stefánsson, V., and Steingrímsson, B.S., 1990: *Geothermal logging I, an introduction to techniques and interpretation* (3rd edition). Orkustofnun, Reykjavík, report OS-80017/JHD-09, 117 pp.

Stefánsson, V., Gudmundsson, Á., and Emmerman, R., 1982: Gamma ray activity in Icelandic rocks. *The Log Analyst, XXIII-6,* 11-16.

Thórdarson, T., and Höskuldsson, Á., 2008: Postglacial volcanism in Iceland. *Jökull, 58,* 197-228.

Trønnes, R.G., 2002: *Geology and geodynamics of Iceland: Reykjavik.* Nordic Volcanological Institute, University of Iceland, 1-19.

APPENDIX I: Details of the methods used in analysis

A total of 550 cutting samples were analysed for this study. Sampling of well cuttings was carried out at the rig concurrently with drilling operations. The cutting samples, collected at 2 m intervals were analysed on site in an effort to obtain information concerning the alteration temperatures. This information is useful, especially to the driller, as it acts as a guide and enables avoidance of situations such as an imminent eruption, collapse of formations, sticking of the drill strings and rapid wearing of bits (Njue, 2010).

During this study the samples were analysed further in the laboratory to provide detailed information regarding the history and future of the geothermal system of interest. Thus, after visual examination, the cuttings were first analysed in a binocular microscope (Olympus SZ12 with a magnification of 7× to 90×). The primary objective of this examination was to identify the lithology, oxidation and extent of alteration grade, intrusives, veins, vein fillings and several alteration minerals. It is important to wash the samples before analysis to remove dust particles and, most importantly, to enhance the visibility of certain minerals, for example, pyrites and certain obscured features. Dilute hydrochloric acid was used to identify carbonates, in particular calcite. However, it was taken into account that drilling cement is also rich in calcium carbonate.

Some clarifications, especially regarding rock type, textures, porosity and some alteration minerals, for example zeolites, after the binocular investigation, were answered during the petrographic microscopic analysis. A Leitz-Wetzlar model petrographic microscope was used for this purpose. Thus, 20 samples selected from different depths in the studied borehole were cut and polished to approximately 2 μm and glued on glass using epoxy. Additionally, this analysis gave specific information particularly on mineral types and sequences in vein and vesicle fillings.

Furthermore, in order to understand in greater detail the alteration zones in the geothermal field under investigations, X-ray diffractometer (XRD) analyses were carried out. This method has proven useful for classifying the various types of clay which, in turn, provide information on the alteration temperatures. In total, twenty three samples from well HE-32 were analysed and interpreted (Appendix II). The procedures of this analysis are also detailed in Appendix II.

The geophysical logs (caliper, neutron-neutron, natural gamma, rate of penetration, weight on bit, temperature and resistivity) were also extensively analysed to make the geological interpretation as accurate as possible. Analyses of these logs give information on the structure, physical properties and performance of the geothermal system penetrated by the well. For example, due to the difference in electrical properties between different formations, the resistivity logs will show lithological variations clearly. On the other hand, the natural gamma log detects the gamma radiation from rocks due to isotopes even though these isotopes are found in very small quantities. The count rate measured by a gamma ray tool at each depth in a borehole is related to the concentration of the radioactive isotopes 40K, 238U and 232Th in the formation outside the well, and defines a quantity that is called the radioactivity of that formation (e.g. Stefánsson and Steingrimsson, 1990, in Mbia 2010). This log is especially helpful in identifying intermediate to acid intrusives as these rocks contain elevated concentrations of the above isotopes compared to basaltic rocks. The neutron logs are used in porosity investigations and can be related to the porosity of the formation. The caliper logs measure the diameter of the well.

Fluid inclusions in quartz and calcite were selected for the fluid inclusion studies. The analysis involves the investigations of homogenization temperatures for trapped fluids in mineral vesicles, thereby giving information on the temperatures at which the minerals formed. The analyses were achieved using a fluid inclusion microscope. Such investigations give a clue on the history, current and future predictions of the behaviour of a geothermal system, important for planning in all geothermal fields. The results of this analysis are detailed in Appendix III.

Some data, for example, lithology, alteration minerals from wells HE-3 and HE 51-drilled on the same well pad as well HE-32, were used for comparative purposes. In normal practice, the relationships in neighbouring wells should be exploited for better understanding of the geothermal system under investigation.

Finally, the data obtained from all the above analyses were compiled and plotted using Log Plot 2007 (RockWare Inc., 2007) software which has a provision for visualising all the investigated data in a graphic model for easy correlation before making conclusions.

APPENDIX II: The procedures for XRD sample preparation, analysis and results

Procedures:

1. Order the samples and number them starting from 1 to X;
2. Fill the sample glass ~1/5 with sample and then fill up to around ¾ with water;
3. Close with gum cap;
4. Shaking for 4 hours in a "shaker machine", take care that the bottles can´t move;
5. Take the samples out of the shaker, put the sample glasses vertical and wait 10-15 min, until the largest particles have settled down;
6. Pipette some drops of the clay water on glass circles, which are also numbered from 1 to X;
7. Let dry until the next day;
8. Samples ready for XRD-analysis.

Analysis:

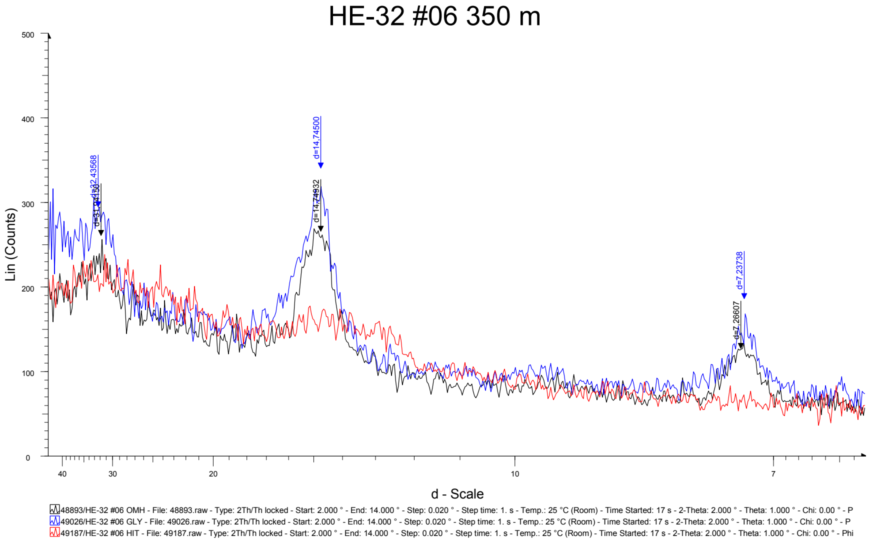

FIGURE 1: Diffractograms of mixed-layer clays at 350 m in well HE 32; peaks at 14.68-14.74 Å are for the untreated (black curve), and the glycolated (blue curve) samples; a collapsed peak (red curve) at 12.33 Å is for the heated sample; and the unchanged peak for all runs at 7.2 Å is for chlorite

FIGURE 2: Diffractograms of chlorite (unstable) at 450 m in well HE 32; peaks at 14.72 and 14.57 Å when the sample is untreated, glycolated and heated and the other at 7.2 Å appears when the sample is untreated and glycolated but disappears completely when heated

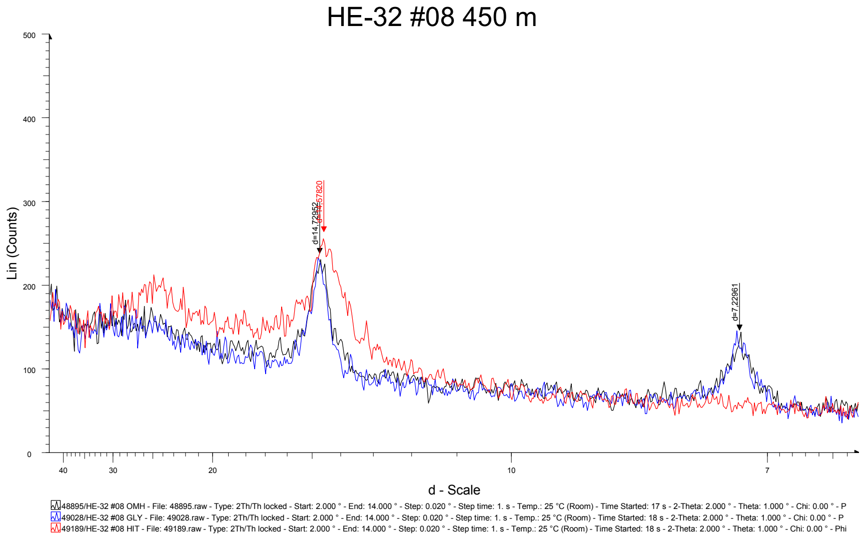

FIGURE 3: Diffractograms of chlorite (stable) at 620 m in well HE 32; peaks are at 14.70-14.86 Å and 7.2-7.3 Å when the sample is untreated, glycolated and heated; the peak at 9.68 Å is for laumontite

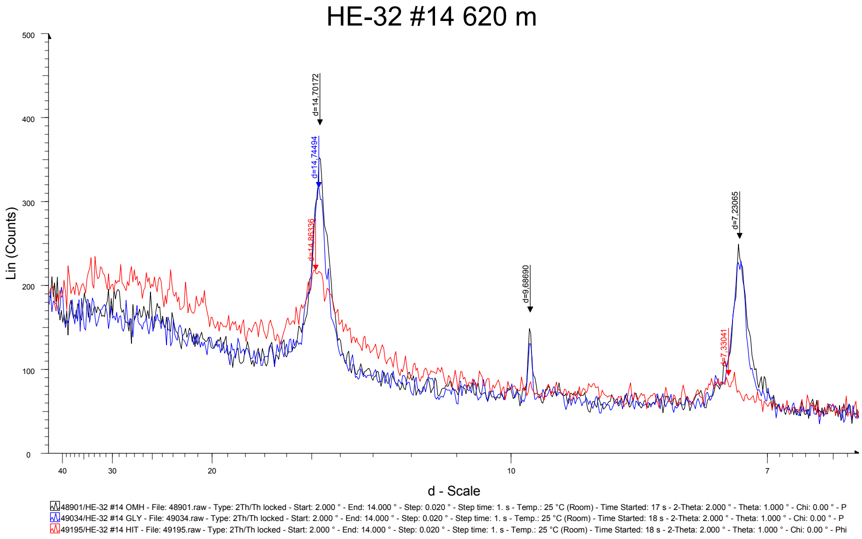

FIGURE 4: Diffractograms of amphibole (probably actinolite) in well HE 32 at 850 m

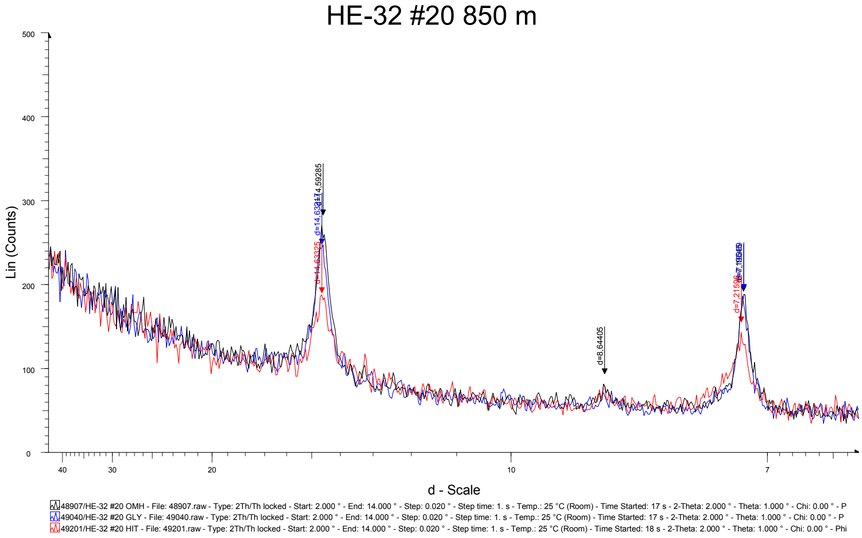

TABLE 1: XRD results

Sample no.	Depth (m)	d(001) Untreated	d(001) Glycolated	d(0001) Heated	Mineral	Remarks
1	106	13.996	14.01	13.996	Smectite	
2	150	14.913	15548	10.013	Smectite	
3	196	13.305	14.817	9.95	Smectite	9.086Å peak of unknown mineral
4	250	13.377	13.76	10.143	Smectite	
5	300	25.050 / 14.684	25.050 / 14.689	14.336/25.477	Mixed-layer clay (MLC)	
6	350	31.492 / 14.749	32.436 / 14.745	0	Mixed-layer clay (MLC)	
7	400	14.674	14.707	14.422	Chlorite unstable	
8	450	14.73	14.731	14.578	Chlorite unstable	
9	500	14.371	14459	14.772	Chlorite unstable	
10	520	14.389	14.451	0	Chlorite unstable	
11	550	14.529	14.544	14.427	Chlorite unstable	
12	570	32.654 / 15.385	32.566 / 15.736	15.105	Chlorite unstable	
13	600	15.208	15.426	0	Chlorite unstable	9.779Å = laumontite
14	620	14.702	14.745	14.863	Chlorite	9.687Å = laumontite
15	650	15.006	14.96	15.392	Chlorite unstable	
16	670	14.769	14.781	14.782	Chlorite	
17	700	14.553	14.548	14.672	Chlorite	
18	720	14.68	14.69	14.771	Chlorite	
19	800	14.808	14.823	14.867	Chlorite	
20	850	14.593	14.632	14.633	Chlorite	8.644Å = Amphibole
21	900	14.441	7.153	14.431	Chlorite	
22	950	15.026	15.014	14.842	Chlorite	
23	1000	14.744	14.872	14.772	Chlorite	8.720Å = Probably amphibole

Appendix III: Results of optical microscopy of thin section analysis for well HE 32

No.	ID no.	Depth (m)	Rock type	Texture	Smec	Cgc	Fgc	Chab	Chalc	Opal	M/S	Cc	Lim	Alb	Pyr	Clay	Qtz	MLC	Wai	Mord	Preh	Laum	Chl	Epi	Wallo
1	19797	30	Tholeeitic basalt	Porphyritic	x																				
2	19798	86	Reworked tuff		x		x						x												
3	19799	170	Basaltic tuff		x	x	x	x			x	x			x										
4	19800	182	Basaltic tuff		x	x	x	x		x	x	x													
5	19801	202	Fine-medium grained basalt	Porphyritic	x							x				x									
6	19802	216	Basaltic breccia	Glomeroporphyritic	x	x	x	x	x	x		x			x										
7	19803	392	Basaltic tuff		x	x	x							x	x		x	x							
8	19804	416	Basaltic tuff		x			x				x			x			x	x						
9	19805	508	Basaltic tuff		x							x						x		x					
10	19806	540	Basaltic breccia	Porphyritic		x						x			x		x	x	x						
11	19807	564	Basaltic breccia	Porphyritic	x							x			x		x	x	x				x		
12	19808	634	Basaltic tuff		x	x						x			x			x					x		
13	19809	662	Basaltic tuff			x						x			x	?x		x					x		
14	19810	706	Basaltic breccia	Porphyritic	x							x			x		x				x	x	x		
15	19811	734	Basaltic tuff									x		x	x		x					x	x		
16	19812	906	Basaltic tuff										x	x	x		x						x	x	
17	19813	1006	Basaltic tuff		x								x				x						x	x	
18	19814	1064	Basaltic breccia	?Porphyritic									x	x			x						x	x	
19	19815	1074	Basaltic breccia	?Porphyritic								x		x			x							x	
20	19816	1100	Basaltic tuff									x	x	x			x						x	x	x

Smec=smectite | Cgc/Fgc=Coarse-grained/Fine-grained clay | Chab=Chabazite | M/S=Mesolite/Scolerite | Cc=Calcite | Lim=Limonite | Alb=Albite | Pyr=Pyrite | Qtz=Quartz | MLC=Mixed layer clay

Phil=Phillipsite | Wallo=Wallostonite | Mord=Mordenite | Preh=Prehnite | Chl=chlorite | Laum=Laumontite | Epi=Epidote | Chalc=Chalcedony | Wai=Wairakite